

**Comparing Paleohydrograph Reconstructions from Subsurface Stratigraphy and
Topography at the Sault Ste. Marie Strandplain**

by

Marcel Rene Heather

A thesis

presented to the University of Waterloo

in fulfilment of the

thesis requirement for the degree of

Honours Bachelor of Science

in

Environmental Science

Waterloo, Ontario, Canada, 2021

© Marcel Heather, 2021

Declaration

I hereby declare that I am the sole author of this thesis. This is a true copy of the thesis, including any required final revisions, as accepted by my examiners.

I understand that my thesis may be made electronically available to the public.

Marcel Heather

Abstract

The Great Lakes are currently at high water levels, which are negatively impacting coastal infrastructure, coastal ecosystems, and stakeholders that rely on the lakes. To better understand natural fluctuations, which includes high lake levels, geoscientists study ancient shorelines to reconstruct paleohydrographs. Reconstructing past lake level elevations from a specific subsurface sedimentary contact or foreshore base (FSB) contact is the most accurate way to gain insight into ancient lake levels. The objective of this thesis is to establish an alternative method to use topographic elevations as a proxy for the FSB in the reconstruction of inferred paleohydrographs from the Sault Ste. Marie (SSM) strandplain. Light detection and ranging (LiDAR) data was used to obtain topographic elevations for this topographic reconstruction. Topographic elevations measured in the field were compared to LiDAR data and these topographic elevations were also compared to FSB elevations measured in cores. Elevation trends and patterns were statistically analyzed and visually analyzed in graph to justify that topographic elevations from LiDAR could be used as a proxy for the FSB or past lake level elevation, but so far this only applies to the SSM strandplain deposited during the Nipissing phase. The field measured topographic swale elevations could be used as an alternative to FSB elevations when a correction factor of 1.49 m was subtracted from each individual swale elevation. LiDAR data was then used to obtain one swale elevation for every beach ridge in the SSM strandplain and then a correction factor of 1.49 m was applied to the LiDAR swale elevations. Results from this thesis found that an inferred paleohydrograph reconstructed from LiDAR swale elevations was an appropriate alternative to infer ancient lake level elevations and trends. However, this has only been shown to apply for the SSM strandplain deposited during the Nipissing phase. Further comparisons at different sites and for different ages of strandplains need to be investigated. In summary, this thesis determined that LiDAR swale elevations can potentially provide an alternative method to reconstruct paleohydrographs, and thus gain valuable insight into natural lake-level trends and patterns to help place current high levels and potential future lake-level fluctuations into context for stakeholders.

Acknowledgements

I would like to thank my supervisor Dr. John Johnston. The guidance and insight he provided over the past eight months for this thesis was invaluable and helped me refine my thesis to be the best possible version I could deliver. His editing and insight into scientific writing helped me reframe how I think about writing and I will carry those lessons into the future.

I would like to thank Dayna Opersko for providing insight into the use of LiDAR data in GIS. Finally, I would like to thank my sister Frances Heather for her help over the past eight months with editing my writing.

Table of Contents

Introduction.....	1
Literature Review.....	4
Objective and Goals.....	10
Methods.....	10
Statistical Analyses.....	11
Cross-strandplain Trend Analysis.....	12
Ages.....	13
LiDAR.....	13
Results.....	14
Field Data.....	14
T-Tests.....	17
Descriptive Statistics.....	18
Cross-strandplain Trend Analysis.....	21
Ages.....	23
LiDAR.....	31
Discussion.....	40
Field Measured Elevation Data Analysis.....	40
Application of Topographic Elevation Data.....	43
LiDAR.....	45
Ages.....	49
Implications.....	49
Conclusion.....	51
Recommendations.....	52
References.....	55
Appendix A: Thesis Design Poster.....	59
Appendix B: Thesis Poster Presentation.....	60

List of Figures

Figure 1. Map of Great Lakes Drainage Basin.....	1
Figure 2. Monthly mean lake level and historic average in Great Lakes.....	3
Figure 3. Strandplain examples.....	5
Figure 4. Cross section of typical beach ridge in Great Lakes.....	6
Figure 5. Plotted field data from the SSM strandplain.....	16
Figure 6. Box plots for SSM strandplain field elevations.....	21
Figure 7. Piecewise regressions.....	23
Figure 8. Calibrated radiocarbon ages of SSM beach ridges.....	29
Figure 9. Field measured elevations versus age of ridges.....	31
Figure 10. Sault Ste. Marie strandplain DEM.....	33
Figure 11. Sault Ste. Marie strandplain elevation profile.....	34
Figure 12. Paleohydrograph of the SSM strandplain including LiDAR swale elevations.....	36
Figure 13. Inferred paleohydrograph for the SSM strandplain site.....	40

List of Tables

Table 1. Summary table of paired t-test results.....	18
Table 2. Descriptive statistics.....	20
Table 3. Radiocarbon age data for the SSM strandplain.....	25
Table 4. LiDAR swale elevation data.....	38

Introduction

The Great Lakes are currently near record high water levels that are negatively impacting infrastructure and causing coastal erosion and flooding along their extensive coastlines (Gronewold & Rood, 2019). The Great Lakes watershed is home to over 30 million people in Canada and the United States, and spans over 1,200 km from west to east, including the University of Waterloo at the center of three of the five lake basins (Figure 1) (Fuller et al., 1995). This transboundary watershed supports a thriving environment and a vital economy and society.



Figure 1. Map of the Great Lakes Drainage Basin. University of Waterloo is located near the center between three of the five lakes of the basin. Modified from IJC (n.d.).

The Great Lakes account for approximately 20% of the world's freshwater, and the millions of residents in the watershed rely on the lakes as a source for their drinking water (Gronewold et al., 2013). Other stakeholders in the Great Lakes watershed include the

shipping, fishing and tourism industries, as well as power generation (Rau et al., 2020). These industries employ millions of people and are the backbone to the economy of this transboundary watershed (Rau et al., 2020).

Fluctuations in the elevation of the water level, either up or down in elevation, within the Great Lakes can negatively impact the many stakeholders within the watershed. For example, the operating costs of shipping vessels could increase a considerable amount if lake levels were to drop significantly as they have done in the recent past (Millerd, 2011). Along with a large economy, the Great Lakes support a thriving ecosystem that will also be impacted by lake-level fluctuations. These fluctuations could potentially reduce beneficial ecosystem services that the lakes provide, for example, wetlands that provide fish breeding habitats could be reduced by large fluctuations (Hartman, 1990). Another negative impact of rising lake levels would be for property owners on the Great Lakes coastlines. As water levels rise, coastal erosion and flooding could increase and pose a risk to coastal properties. Properties could shrink as the water level rises and infrastructure could be damaged or lost. Having insight into the fluctuations of lake levels will give these stakeholders context for modern lake levels and help them be prepared for potential future fluctuations so they can continue to thrive.

Lake levels of the Great Lakes have been recorded since the mid-1800s, providing a useful historic record (Gronewold et al., 2013). The modern recording of lake levels is done by water-level gauges that are installed across all five lakes in both Canada and the United States (Gronewold et al., 2013). The data collected from these gauges provides insight into modern lake levels by showing variations and averages over recent history (Figure 2). The gauges record lake levels that are heavily influenced by human activities, but do not provide the whole picture of Great Lakes water level fluxes. This is because the time period of some

fluctuations are beyond the length of the gauge record, and also because human impacts are occurring at the same time as natural fluxes.

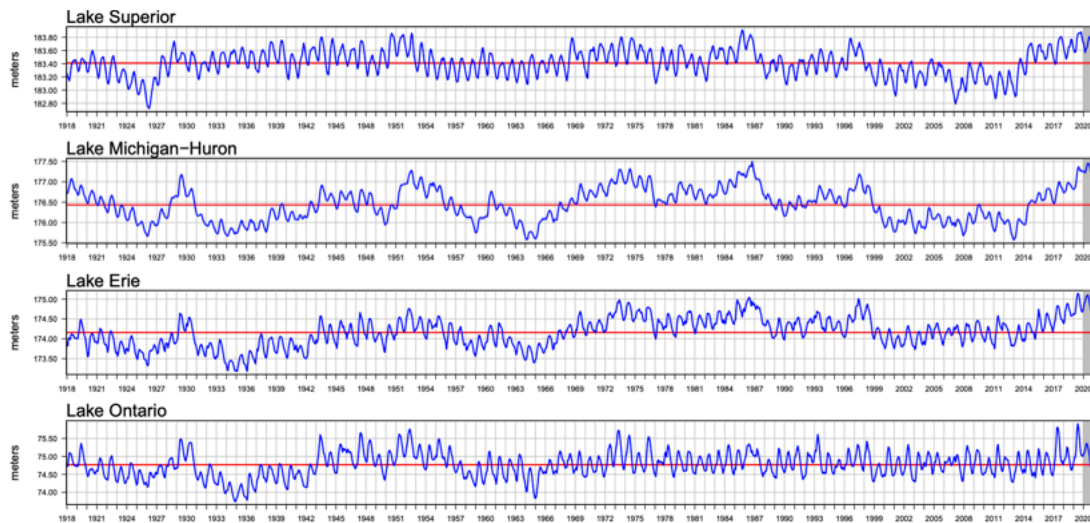


Figure 2. Monthly mean lake level and historic average in Great Lakes. Includes lakes Superior, Michigan-Huron, Erie, and Ontario since 1918. Note the relatively steep increase during the last seven years in lakes Superior, Michigan-Huron, and Erie (USACE, 2020).

The modern water levels that the gauges record includes natural fluxes, but due to the anthropogenic impact on the Great Lakes it would be nearly impossible to separate the natural and anthropogenic trends and patterns from each other. A record that goes back into geologic time before large anthropogenic impacts is required to observe the natural fluxes of the Great Lakes. By knowing the ancient natural trends and patterns separately from anthropogenic ones, the modern fluctuations can be understood to a greater depth. This knowledge could reveal what parts of modern fluctuations are caused by natural fluxes. An insight into the natural and modern trends and patterns can provide context to understand modern high lake levels and may help create realistic scenarios for stakeholders to plan for future potential natural and anthropogenic fluxes.

Literature Review

Ancient lake levels are recorded in beach ridges that were formed at the time their respective lake level occurred (Thompson, 1992). Over time these ancient beaches were preserved when subsequent beach ridges formed in front of them and the shoreline prograded, creating strandplains (Figure 3) (Otvos, 2000). These strandplains create a lateral chronosequence of preserved ancient beach ridges. Within the Great Lakes strandplains, beach ridges preserve ancient lake levels from the late Holocene (Johnston et al., 2014). There have been many variable approaches used in the past that attempted to reconstruct the ancient lake levels recorded in Great Lakes strandplains. The relationship between what was measured in the field and interpreted as lake level was not consistent or accurate. The lack of accuracy and consistency prevented reconstructions from being truly representative of ancient lake levels. One example of this is in Larsen (1994), where topography and stratigraphy were used as indicators of ancient lake levels. Multiple contacts from within the sediments were used and these contacts were not all directly related to ancient water levels. To obtain a better understanding of lake levels, a method that is more consistent and accurate was required.

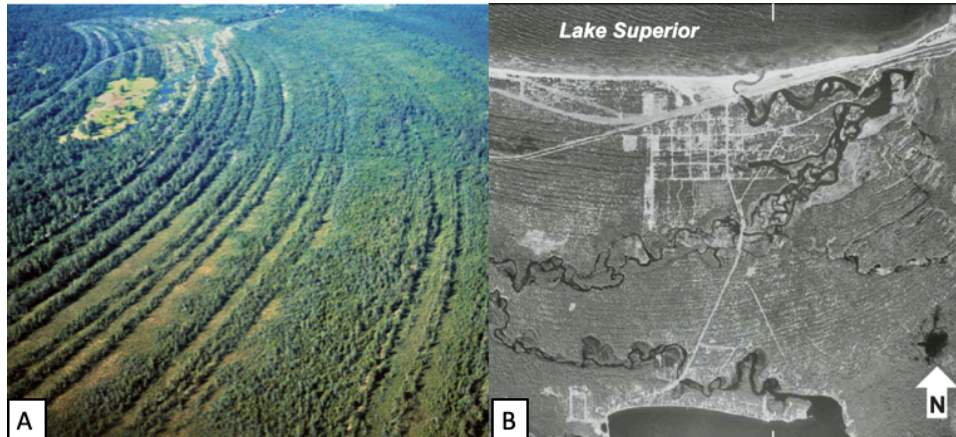


Figure 3. Two examples of strandplain topography. A) Photo of a strandplain near Manistique, Michigan along the coastline of Lake Michigan. Beach ridges are covered with trees and wetlands are between beach ridges. B) Au-Train Bay strandplain aerial photo. Beach ridges are light coloured linear features covered in trees (Wilcox et al., 2007 and Johnston et al., 2007).

Each beach ridge within a strandplain contains a subsurface sedimentary contact that records the elevation of an ancient lake level (Johnston et al., 2014). The subsurface contact that records the ancient lake level is the foreshore base (FSB) contact, this contact records the ancient lake level because the sediments of the foreshore are water-lain (Figure 4) (Thompson, 1992). This sediment and contact can be observed at water level on a modern beach where the beach sand at water level has a steep dip downward to coarser sediment. A new and consistent approach to reconstruct ancient lake levels was developed using the FSB contact and improved upon the inconsistent and inaccurate methods used previously. This method was developed in Thompson (1992). In this method, the beach ridge of interest is vibracored and the sediments in the core are analyzed for grain size distribution as well as physical structures (Thompson, 1992). The contact is found by using the grain size and physical characteristics that are representative of the foreshore, and then elevation is determined by using the elevation of the

core site and then subtracting the depth of the contact found within the core itself as described in Thompson (1992).

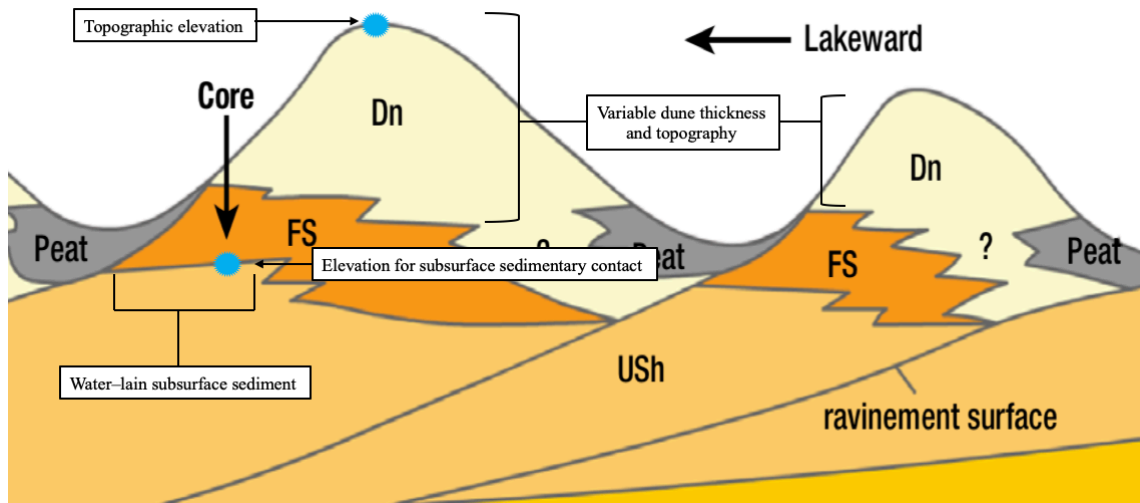


Figure 4. A cross section of a typical beach ridge within the Great Lakes. Aeolian, Dn: dune. Water-lain, Fs: foreshore, Ush: upper shoreface. Locations of where elevation data is collected is denoted with blue star symbols. Note the difference in elevation between subsurface contact and topography as well as variable topography of dunes. Modified from Johnston et al. (2014).

To reconstruct a paleohydrograph the elevation and age of multiple beach ridges from within a strandplain are required. In the Thompson (1992) method, the elevation is obtained from the FSB contact as described previously. The age of the ancient lake level was previously based off of peat, or organic rich sediments from near the location of the core that were assumed to have formed between the ridges immediately after time of deposition of the subsurface contact (Thompson, 1992). This was an inaccurate method to obtain ages as the organic sediments are not directly related to the subsurface contact and their age may not be representative of time of deposition. A more accurate dating method was developed where optically stimulated luminescence (OSL) is used to date the sediments from around the subsurface contact itself (Argyilan et al., 2005). To complete the paleohydrograph, glacial isostatic adjustment (GIA)

must also be considered. The rate of surface adjustment post glaciation can be different between sites, therefore applying the respective GIA to the sites allows them to be a true representations of ancient lake levels (Johnston et al., 2014). Using the elevation method of Thompson (1992), applying ages collected with OSL methods described here, and applying proper GIA to the elevations is accepted to be the most accurate method to reconstruct paleohydrographs.

Thompson's (1992) method has been applied in many papers at multiple strandplain sites within the Great Lakes. In Thompson and Baedke (1997), and Baedke and Thompson (2000), this method was applied in Lake Michigan strandplains. Both of these papers used the subsurface contact method to obtain elevations and make lake-level curves, and discover information regarding GIA. In Thompson and Baedke (1997) quasiperiodic lake-level fluctuations were established by using paleohydrographs reconstructed with the subsurface contact method. In Johnston et al. (2012) the subsurface contact method of obtaining elevations was applied to sites in Lake Superior. Johnston et al. (2012) used the reconstructed paleohydrographs to establish a lake level record in relation to the Lake Superior outlet. The multiple applications of the Thompson (1992) method demonstrates that obtaining elevations from the subsurface sedimentary contact for paleohydrograph reconstruction is the most accurate way to decipher past natural trends and patterns of lake level changes. Paleohydrographs reconstructed in this manner can reveal multi-decadal to millennial scale trends and patterns in ancient lake-level fluctuations.

Although the subsurface stratigraphic contact method is widely accepted to be the most accurate method to obtain elevations for paleohydrographs, there is an opportunity to revisit using topography as a method to reconstruct ancient lake levels. The major difference between using strandplain topography and the FSB contact to reconstruct paleohydrographs is in how the

two were deposited. The FSB contact is a water-lain sediment that is directly related to lake level (Thomson, 1992). Alternatively, topographic elevation is from aeolian dune sediments that could have formed at different times than the FSB contact. The aeolian processes which form the dune caps can be inconsistent and cause variable elevations and topography of the beach ridges (Tamura, 2012). Dunes will therefore show inconsistent morphology and elevations compared to the water-lain FSB contact (Figure 4). The variation in the dune morphology could also be caused by post-depositional changes. The dune cap of a beach ridge is exposed to weather and vegetation which can affect the ridges elevation, making it a less accurate representation of its original depositional environment (Tamura, 2012). The FSB contact would be less susceptible to post depositional changes since it is buried and protected from overlying sediments. This difference in consistency of the elevations will require a correction factor or multiple factors to account for the inconsistency and inaccuracy of topography.

One recent application that briefly used the topographic method to reconstruct a paleohydrograph was in Johnston et al. (2012). In this paper, a consistent relationship was found between topographic elevation and the elevation of the subsurface contact within strandplains (Johnston et al., 2012). This relationship was on average a two-meter difference in elevation (Johnston et al., 2012). The average difference of two meters was used as a correction factor that was applied to the entire strandplain to bring topographic elevations down closer to the water-lain subsurface sedimentary contact (Johnston et al., 2012). Applying the correction factor involved subtracting the factor from the topographic elevation (Johnston et al., 2012). After applying this correction factor, it was found that there were similarities between paleohydrographs reconstructed using topographic elevations and the elevations of the subsurface contacts (Johnston et al., 2012).

The use of topographic elevation in Johnston et al. (2012) creates an opportunity to further explore the use of topographic elevations as a method to obtain ancient lake levels. The application of a single correction factor to make topographic elevations closer to those of the FSB contact provide a starting point for this opportunity. However, the use of one correction factor may not be realistic for all sites, as there is variation in topography across different strandplains (Figure 4). To accurately represent multiple beach ridges and multiple strandplain sites, trends and patterns in the difference between topographic elevation and the elevation of the FSB contact within a strandplain and across multiple strandplains will need to be found. By accounting for these trends and patterns the correction factor(s) can be established and applied to the strandplain sites to make topographic elevations a more accurate representation of lake level.

Topographic data can be collected in many ways including field surveys, aerial photographs, and topographic maps. One of the most accurate ways to remotely obtain topographic data is through light detection and ranging (LiDAR) (NOAA, 2012). The method of obtaining LiDAR data involves flying a plane over the area of focus that emits beams of light and calculates ranges based on return times of the light reflections (NOAA, 2012). The remote nature of LiDAR is beneficial because it provides detailed information for a field site without the challenges of completing field work. LiDAR is also easily accessible and available on government websites, including LiDAR data of the Great Lakes coastal areas in the United States. There is a high potential for the use of LiDAR for strandplains since LiDAR can resolve beach ridges within 15cm of vertical accuracy (Sallenger et al., 2003). The use of a correction factor on topographic elevations to allow them to better reflect the subsurface contact in Johnston et al. (2012) creates an opportunity to further explore using the topographic method. By

providing accurate remote topographic data, LiDAR helps with the potential to create paleohydrographs from topography to compare with subsurface stratigraphic paleohydrographs.

Objective and Goals

The objective of this project is to evaluate the use of paleohydrographs reconstructed from topography to represent ancient lake levels. This will be done by comparing paleohydrographs from topography with paleohydrographs from subsurface stratigraphy, both reconstructed from the same landforms at the Sault Ste. Marie strandplain. This comparison will aim to determine if paleohydrographs derived using topography or surface elevations can be used to accurately represent the elevation of ancient lake levels associated with individual beach ridges in strandplains. Recommendations for the use of paleohydrographs from topography will be made along with any correction factor(s) that is/are required for the topographic paleohydrograph to accurately represent ancient lake level.

The main goal of this thesis will be to reconstruct a paleohydrograph from topography for the SSM strandplain deposited during the Nipissing phase. A correction factor may be needed, and applied to topographic elevations to be similar to paleohydrographs derived from subsurface stratigraphy. By establishing the correction factor(s), guidelines will be created for the application of paleohydrographs from topography in strandplains. Developing guidelines for the use of topography from LiDAR data to reconstruct paleohydrographs will create new potential opportunities of reconstructing ancient water level trends and patterns for areas that have not been cored and have not had field work completed but have been age dated.

Methods

To reconstruct a paleohydrograph, an elevation from a beach ridge representative of an ancient lake level, and an age for the time that ancient lake level occurred are required.

Elevations and ages for the Sault Ste. Marie (SSM) strandplain were obtained from Johnston et al. (2012). The FSB elevations were collected from the water-lain subsurface stratigraphic contact within the beach ridges as described in Thompson (1992). These elevations were related to the International Great Lakes Datum of 1985 (IGLD85) by surveying between the current lake level, recorded by water level gauges and the ground surface where the cores were taken (Coordinating Committee on Great Lakes Basic Hydraulic and Hydrologic Data, 1995).

Topographic elevations for the swales and ridge crests were also collected in the SSM strandplain (Johnston et al., 2012). The organic samples used for radiocarbon dating that provide relative ages for the strandplain were collected from the base of the wetlands found in the swales between ridges. In this thesis the topographic ridge crest and swale elevations as well as the FSB elevation data from Johnston et al. (2012) were graphed together to recreate part of figure 9 in Johnston et al. (2012) and develop a method to recreate a paleohydrograph inferred from topography. Distance landward of the ridge crests was used as the independent variable and the corresponding elevations of the ridge crest, swale, and FSB as the dependent variables.

Connecting each data point together using a linear interpolation helped create two separate cross-strandplain elevation trends and a relative paleohydrograph. The resulting cross-strandplain elevation trends were visually analyzed to determine if there were any similarities between the ridge crest and swale elevation trends and the FSB relative paleohydrograph.

Statistical Analyses

The elevation data from Johnston et al. (2012) for the SSM strandplain was analyzed to determine if there were similarities between the ridge crest and swale elevations and the FSB elevations. The first statistical test done was two separate paired t-test that compared the range of elevations of the ridge crest to the FSB elevations as well as the range of swale elevations to the

FSB elevations. This test was done to determine if there was a statistically significant difference between either the ridge crest elevations or the swale elevations and FSB elevations. The next analysis that was done was finding the descriptive statistics of the calculated differences between the ridge crest and FSB elevations and the swale and FSB elevations. The FSB elevations were subtracted from their corresponding ridge crest and swale elevations to obtain two ranges of differences between the topographic and subsurface elevations. The descriptive statistics of these ranges were calculated. The descriptive statistics included the quartiles, range, mean, median, and standard deviation. Box plots representative of the ridge crest to FSB elevation difference and swale to FSB elevation difference were created to compare the elevation differences. The mean difference between the elevations that were most accurate to the FSB and the FSB elevations was then used to obtain a potential correction factor for the corresponding topographic elevations.

Cross-strandplain Trend Analysis

The following methods analyzed only the swale elevations and their relation to the FSB elevations, this was done because the statistical analyses determined the swale elevations were the most accurate topographic elevations compared to the FSB elevations. The swale cross-strandplain elevation trend and FSB relative paleohydrograph were divided into two sections, this was done at five separate cores and linear regressions were created for each of the four sections. This was done because at distance landward of 400m there is a visible change in the trend of the FSB relative paleohydrograph and the cross-strandplain elevation trends. The division at core 1218 was chosen to analyze further since the regressions of the four separate sets of elevations showed the most similarities between the swale elevations and the FSB elevations.

The slopes and R-squared values of these regressions were then compared to determine similarities between the FSB elevations and swale elevations.

Ages

The ages from Johnston et al. (2012) were graphed against their corresponding samples distance landward. A linear regression was created through this scatter plot to create an age model for the strandplain data to assign an age for every ridge. This age model was applied to the swale cross-strandplain elevation trend and the FSB relative paleohydrographs by using each individual elevations distance landward as the horizontal value in the models equation to replace distance landward with calendar year BP. The new cross-strandplain elevation trend and relative paleohydrograph with age BP as the independent variable were visually analyzed for trends and patterns. The trends and patterns seen in the elevations should be the same as seen in the statistical analysis because the age model only changed the horizontal values and made no changes to the vertical elevation values.

LiDAR

A relative paleohydrograph was reconstructed using LiDAR data to obtain the topographic elevation values. LiDAR data was obtained from the NOAA digital coast, this data contained LiDAR ground points for the study site (NOAA Digital Coast Data Access Viewer, 2021). The LiDAR ground points for the study site were converted into a digital elevation model (DEM) raster layer to help resolve individual ridges and to create continuous elevations for the site. A transect line that extends approximately perpendicular to ridge crests and across the largest distance between ridges was created from the DEM. The ridge crests that were visible on the DEM and were observed along the transect were counted to provide the number of swales that will occur between them, and the distance from the most lakeward side of the transect to the

individual ridge crests were measured and recorded to mimic methods of coring locations during fieldwork. A topographic profile that extends along the transect was generated. The recorded distances of the visible ridges on the DEM were used to determine the location of their corresponding ridge crests along the cross section. The elevation and distances of the swales were then chosen to be the lowest elevation point between two known ridge crests, in the case where two ridges were separated by a long distance and by many different low points the mid-point was found and the lowest point closest to that mid-point was used for elevation. The elevation of the ridges was found at a single point along with that points corresponding distance landward. The elevations were converted to the IGLD 85 datum and graphed as a paleohydrograph with distance landward versus elevation (Coordinating Committee on Great Lakes Basic Hydraulic and Hydrologic Data, 1995).

The mean difference between the swale elevations and FSB elevations from Johnston et al. (2012) was used as a correction factor for the LiDAR swale elevations. This correction factor was subtracted from the individual LiDAR swale elevations to create a cross-strandplain elevation trend that is a proxy for the FSB relative paleohydrograph and is also representative of ancient lake levels. The corrected swale elevations were then visually compared to the FSB relative paleohydrograph to ensure the LiDAR swale elevations were a relatively good proxy to the FSB elevations needed to recreate a relative paleohydrograph for the SSM strandplain.

Results

Field Data

A paleohydrograph was reconstructed using the elevations measured in the field of the ridge crest, swale and subsurface FSB contact versus the distance landward from the modern shoreline, relative to the IGLD85 datum in meters (Figure 5). Figure 5 shows relative

topographic or surface elevations (ridge crest and swale) and subsurface elevations (FSB). The most accurate approximation of past lake level elevations are the FSB elevations. However, the elevations have been vertically adjusting since their formation by the process of GIA. Therefore, FSB elevations are collectively referred to as a relative paleohydrograph, applicable only to the SSM strandplain or that specific location in Lake Superior. Straight lines are used to connect the data points to reduce unknown inferences, and to keep interpolations simple between the measured points. Figure 5 shows that both the ridge crest and swale elevations follow a similar overall cross-strandplain trend compared to the FSB elevations, but the swale elevations are more consistent with less variation. This is seen in Figure 5 where the ridge crest cross-strandplain trends have frequent inflections between individual points. These inflections would not accurately represent lake-level fluctuations as they are not seen in the FSB cross-strandplain trend. The swale elevations follow the patterns seen between individual FSB elevations more closely than the ridge crest elevations and has less inflection points that don't match the FSB relative paleohydrograph. The less variable swale cross-strandplain elevation trend better reflects the FSB relative paleohydrograph than the ridge crest cross-strandplain elevation trend does. This shows that swale elevations would be the best option to reflect the elevation of ancient lake levels, however these elevations are consistently higher.

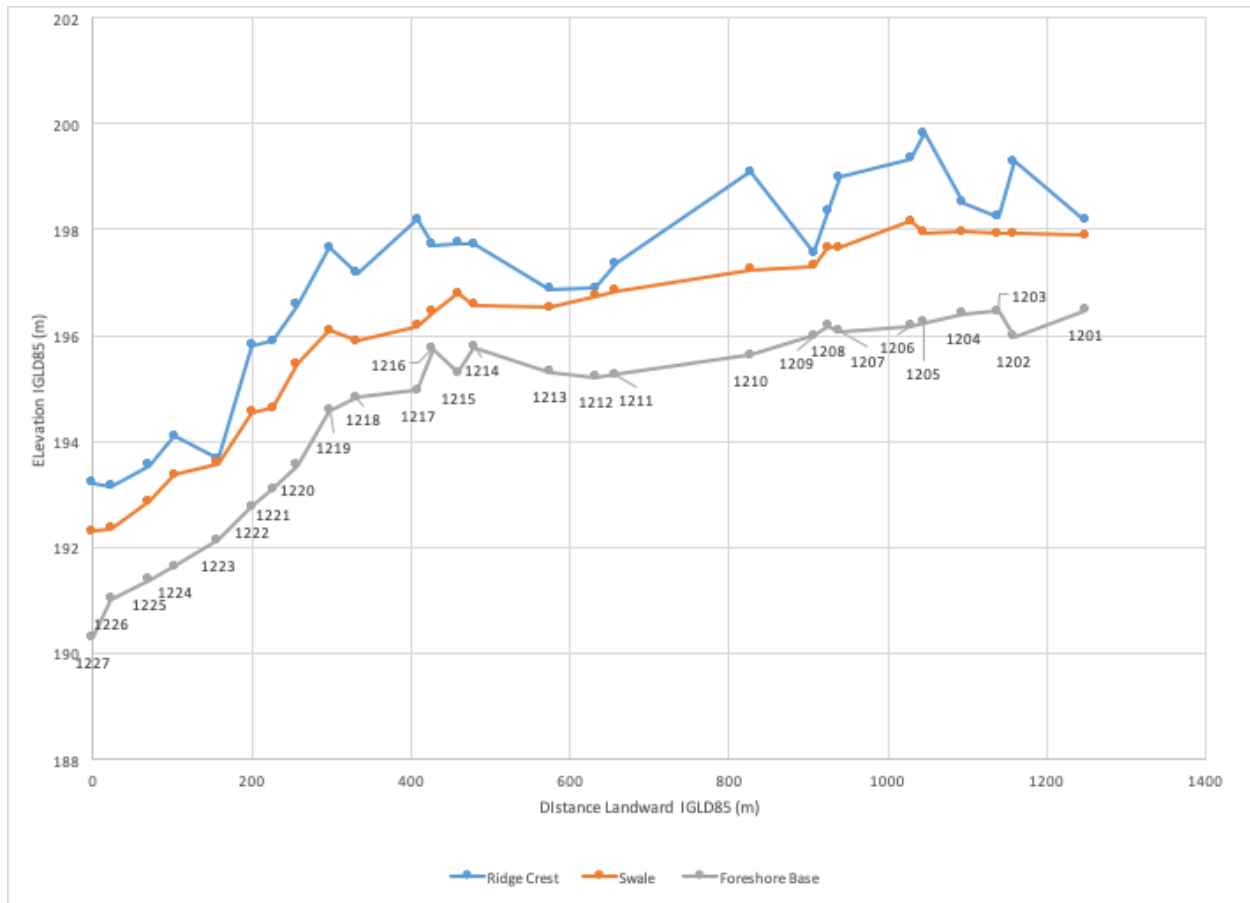


Figure 5. Plotted field data from the SSM strandplain. This includes topographic elevations surveyed from ridge crests and intervening swales, and subsurface elevation of FSB contacts collected from vibracores through ridges (Johnston et al., 2012). Data points of FSB relate to ancient lake levels and collectively form a relative paleohydrograph for the SSM strandplain with labelled vibracore numbers.

Analyses were completed for data from the SSM strandplain to determine if there were similarities in the trends and patterns observed in the cross-strandplain elevation trends and FSB relative paleohydrograph reconstructed from topography and subsurface stratigraphy. These analyses focused exclusively on relict shorelines that formed during the Nipissing phase at SSM and therefore may not be directly applicable to other lake phases (i.e. Algoma), or strandplain sites. Topographic elevations of ridge crests and swales at SSM were compared to the previously

established (Johnston et al. 2012), more accurate representation of ancient lake levels, which is the FSB contact elevation. To compare surface and subsurface elevations, t-tests were completed to determine if the differences between the different sets of elevation data were statistically similar. Box plots were created to help visibly compare datasets. Relative paleohydrographs were reconstructed from surface and subsurface data to explore for trends, patterns and elevation differences across the entire SSM strandplain.

T-Tests

A paired t-test was used to compare field-measured elevations. The elevations being compared were two separate sets of topographic elevations of ridge crests and swales from surveying and FSB elevations from surveying and coring. A paired t-test was used because the individual elevations were associated with similar ridges and therefore represent multiple elevation measurements from one strandplain or one population. The paired t-test showed that the field measured ridge crest and swale elevations were significantly different than the FSB elevations (Table 1).

Table 1. Summary table of paired t-test results. The ridge crest column and swale column represent two separate paired t-tests with the FSB column. P(T<=t) two tail row shows statistically significant difference results of both of the paired t-tests.

	Ridge Crest	Swale	FSB
Mean	197.05828	196.1060622	194.6114133
Variance	3.890557063	3.387165222	3.565313763
Observations	27	27	27
Pearson Correlation	0.944884701	0.985945887	
Hypothesized Mean Difference	0	0	
df	26	26	
t Stat	19.6739614	24.5643001	
P(T<=t) one-tail	1.94423E-17	8.05946E-20	
t Critical one-tail	1.70561792	1.70561792	
P(T<=t) two-tail	3.88846E-17	1.61189E-19	
t Critical two-tail	2.055529439	2.055529439	

Descriptive Statistics

An analysis of the calculated differences between the field measured topographic elevations of the ridge crests and swales to the FSB at the SSM site has shown that within the study site, the topographic elevation of the swales within the strandplain have a consistent difference in elevation with the FSB contact elevation when compared to the elevation difference between the ridge crest and the FSB (Figure 5). The mean elevation difference between the swale

and the FSB was 1.49 m with a standard deviation of 0.32 m and a range of 1.28 m (Table 2). For the SSM strandplain the elevation difference between the swale and the FSB had a smaller standard deviation, 0.32 m versus 0.65 m, and range, 1.28 m versus 2.06 m, than that of the ridge crest and the FSB, respectively (Table 2). The swale to FSB difference was also more symmetrically spaced around the median when compared to the box plot for the ridge crest to FSB difference (Figure 6). The smaller and more symmetrical deviation around the median demonstrates that the swale elevation would be more appropriate to use as a proxy for FSB elevation within the SSM strandplain than the ridge crest elevation would be. The ridge crest elevation is more variable and less consistent with the FSB. However, the swale elevation is elevated somewhat consistently from the FSB elevations. To help infer an FSB elevation from a swale elevation one must subtract a value or values from swale elevations. Because the swale elevations are somewhat consistent with FSB elevations, applying an average value was chosen. A value of 1.49 m was used for the SSM strandplain as a specific correction factor. To use this correction factor, the value of 1.49 m was subtracted from the topographic swale elevations, resulting in a more accurate representation of ancient lake levels than the swale elevations alone, inferred from topography.

Table 2. Descriptive statistics. Descriptive statistics are for the difference in elevation between the ridge crest and FSB and between the swale and FSB. The swale to FSB elevation comparison has smaller standard deviation and range than the ridge crest to FSB elevation comparison.

Ridge Crest - FSB		Swale - FSB	
Mean	2.45	Mean	1.49
Std. Deviation	0.65	Std. Deviation	0.32
Minimum	1.52	Minimum	0.71
Quartile 1	1.96	Quartile 1	1.37
Median	2.35	Median	1.51
Quartile 3	3.03	Quartile 3	1.65
Maximum	3.58	Maximum	1.99

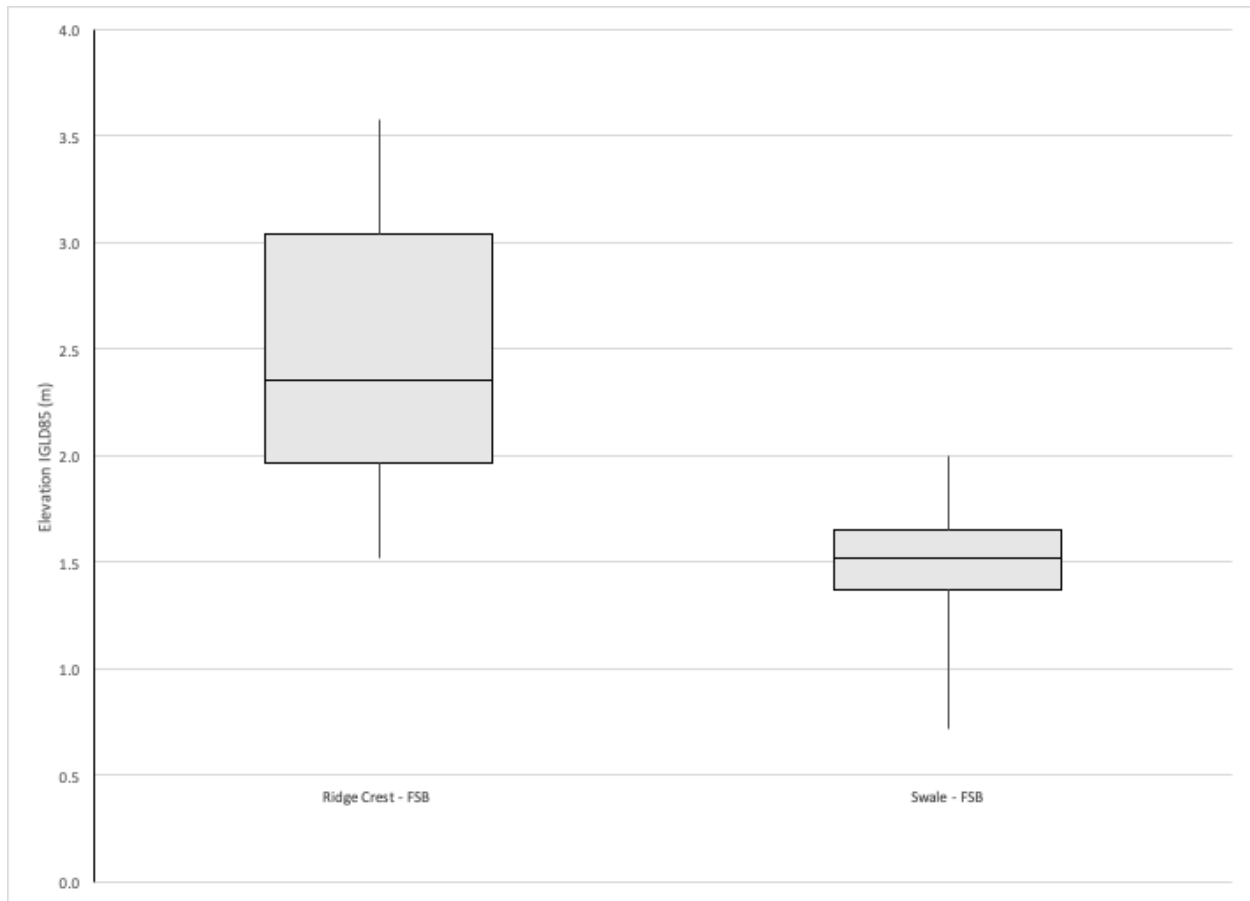


Figure 6. Box plots for SSM strandplain field elevations. Box plots show the differences between the ridge crest elevation and swale elevation with the foreshore base elevation. The swale to FSB box plot shows smaller and more symmetrical deviation than that of the ridge crest to FSB box plot.

Cross-strandplain Trend Analysis

Within Figure 5 there is a change in the cross-strandplain elevation trend reconstructed from swale elevations and the FSB relative paleohydrograph at approximately 400 m landward. On the landward side of 400 m the cross-strandplain trend and relative paleohydrograph become more level than the lakeward side of 400 m, where the trend is steeper. The change observed at 400 m landward could potentially be seen as a point of change in the rate of change of relative lake level, even though this is distance and not age. To determine if the swale elevations

accurately reflected the FSB elevations on both sides of 400 m landward the cross-strandplain elevation trend and relative paleohydrograph were divided into two separate front and back sets of elevations at core 1218. Core 1218 is included as the last point of the front sets of the elevation, because it provided the best alignment of linear regressions with the plotted elevation data.

After splitting the trends into front (lakeward) and back (landward) sets, linear regressions were made to visualize the two individual elevation trends in each set (Figure 7). The four regression lines were a relatively good fit, shown by the relatively high R-squared values for the swale and FSB elevations at 0.971 and 0.977 respectively for the lakeward sets, and 0.911 and 0.722 respectively for the landward sets. The regression slopes for the swale cross-strandplain elevation trend and FSB relative paleohydrograph were 0.0121 m/m and 0.0129 m/m respectively for the front set of elevations and 0.0022 m/m and 0.0014 m/m respectively for the back set of elevations. Five different piecewise regressions were done with the midpoint being changed from core 1215 to 1219. Splitting the trends at different cores was done to determine if there were any cores where there were visible differences in the sets of elevations, and also to determine which core was the best to divide the trends at. In these different tests it was found that splitting the cross-strandplain elevation trend and relative paleohydrograph at core 1218 provided the highest R-squared values and slopes that were the most similar to each other. The high R-squared values show their respective regressions and regression slopes accurately reflect the overall trend of the field-measured elevations. The observed similarity in slopes between the swale elevations and FSB elevations in the front and back sets show that the swale elevations are an appropriate proxy for FSB elevations on either side of the observed point of change in the cross-strandplain trend. Therefore, a single correction factor can be used to correct

the swale elevations for the SSM strandplain since the swale cross-strandplain trend most closely reflects the FSB relative paleohydrograph across the entire strandplain.

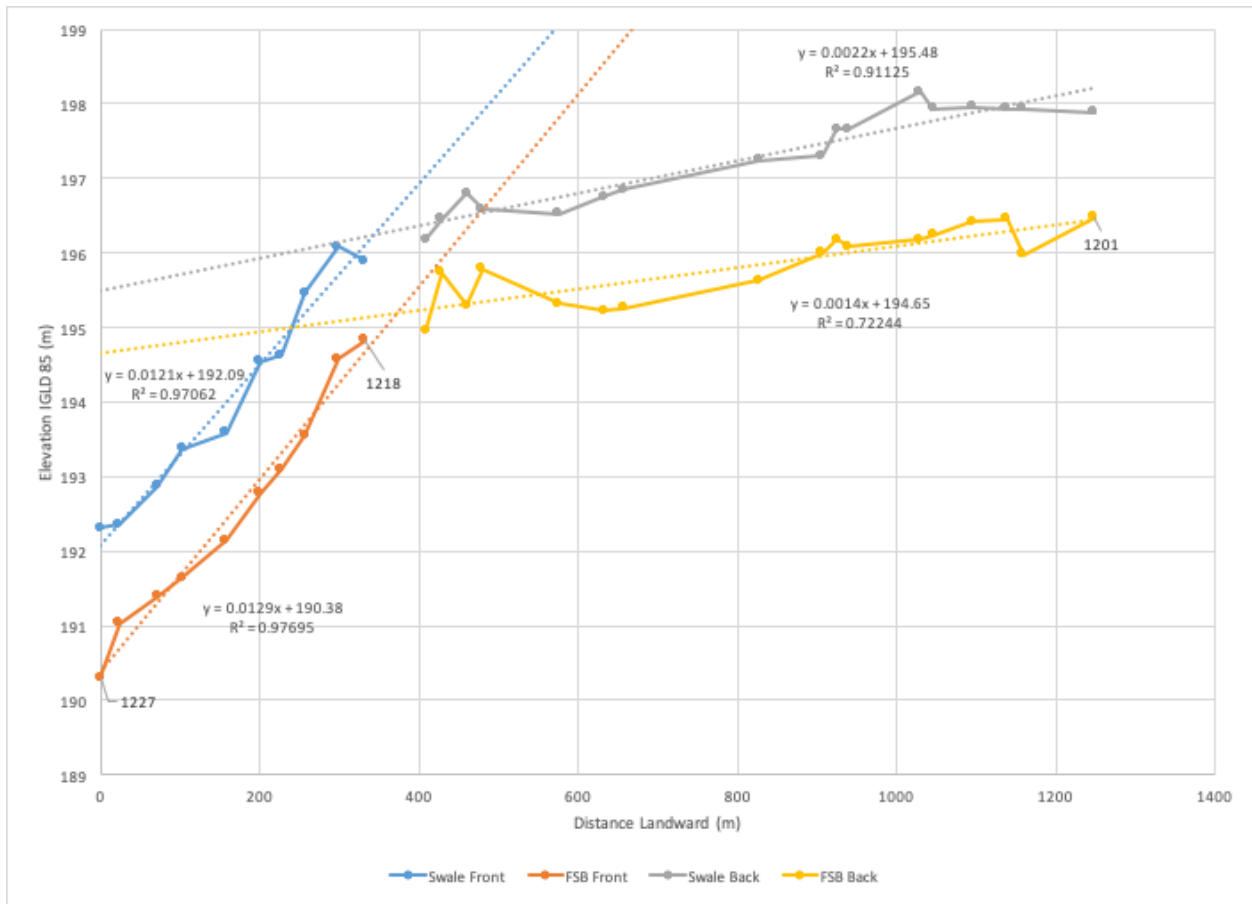


Figure 7. Piecewise regressions. Regressions are of the swale cross-strandplain elevation trend and FSB relative paleohydrograph. Reconstructed from swale and FSB elevations. All four regressions show relatively high R-squared values for each set of elevations and slopes that are similar to each other between the swale and FSB regressions.

Ages

Radiocarbon ages were obtained from Johnston et al. (2012). The sediments that were collected for age dating the SSM study site were collected from the bottom of wetland sediments found in the swale areas between ridges. The distance landward of these samples was recorded. The reported ages from Johnston et al. (2012) were recalibrated using the CALIB program due to

there being a change in calibration values since 2012 (Table 3) (Stuiver et al., 2021). These values were then graphed versus the distance landward of their respective samples (Figure 8). Three samples (lab codes: GX30560, GX30559, and GX30558), were removed from the analysis and not graphed because they seemed to be outliers and plotted much older than the majority of the ages further landward in the SSM strandplain. The cross-strandplain trend in ages also helped identify outliers. The ridges closer to the modern shoreline should be younger than the ridges further landward within the study site because the landward ridges would have to form before the subsequent ridges were able to form. The three most lakeward samples did not follow this expected trend, necessary to make geologic sense in strandplain formation and therefore were removed from the graph to avoid them incorrectly influencing the age model that was created for the study site. Variability in radiocarbon ages collected in other Lake Superior strandplains has also been identified by Johnston et al. (2012) and are problematic when creating age models from radiocarbon ages.

Table 3. Radiocarbon age data for the SSM strandplain. Original ages collected in Johnston et al., (2012). Ages recalibrated using CALIB program (Version 8.2html; Stuiver et al., 2021) to account for change in calibration values since 2012.

Lab Code	Distance (m)	Reported Age	Calibrated two sigma age range	Relative area under distribution	Median Probability	Johnston et al. (2012) Median Probability	Difference in Calibrated Ages
GX-30560	23	3300+/-70	3379 - 3652	0.94	3528	3533	5
GX-30559	103	3760+/-80	3921- 3951	0.034	4131	4133	2
GX-30559	103	3760+/-80	3958 - 4359	0.923	4131	4133	2
GX-30559	103	3760+/-80	4365 - 4405	0.037	4131	4133	2
GX-30558	158	3900+/-90	4005 - 4033	0.011	4321	4324	3
GX-30558	158	3900+/-90	4082 - 4573	0.989	4321	4324	3
GX-30557	227	2170+/-60	2002 - 2031	0.058	2170	2182	12

Table 3. Continued.

Lab Code	Distance (m)	Reported Age	Calibrated two sigma age range	Relative area under distribution	Median Probability	Johnston et al. (2012) Median Probability	Difference in Calibrated Ages
GX-30557	227	2170+/- 60	2038 - 2327	0.942	2170	2182	12
GX-30556	332	1470+/- 60	1287 - 1422	0.884	1359	1367	8
GX-30556	332	1470+/- 60	1448 - 1476	0.049	1359	1367	8
GX-30556	332	1470+/- 60	1484 - 1516	0.051	1359	1367	8
GX-30555	479	1720+/- 70	1412 - 1463	0.053	1612	1634	22
GX-30555	479	1720+/- 70	1466 - 1743	0.947	1612	1634	22
GX-30554	575	1890+/- 70	1623 - 1668	0.055	1805	1830	25
GX-30554	575	1890+/- 70	1693 - 1949	0.912	1805	1830	25

Table 3. Continued.

Lab Code	Distance (m)	Reported Age	Calibrated two sigma age range	Relative area under distribution	Median Probability	Johnston et al. (2012) Median Probability	Difference in Calibrated Ages
GX-30554	575	1890+/- 70	1959 - 1989	0.033	1805	1830	25
GX-30553	657	3070+/- 70	3073 - 3407	0.98	3271	3278	7
GX-30553	657	3070+/- 70	3425 - 3445	0.02	3271	3278	7
GX-30552	827	3590+/- 90	3640 - 3668	0.019	3896	3897	1
GX-30552	827	3590+/- 90	3683 - 4104	0.95	3896	3897	1
GX-30552	827	3590+/- 90	4106 - 4149	0.03	3896	3897	1
GX-30551	939	3800+/- 80	3976 - 4416	0.998	4193	4195	2
GX-30550	1046	3330+/- 70	3396 - 3434	0.04	3558	3565	7

Table 3. Continued.

Lab Code	Distance (m)	Reported Age	Calibrated two sigma age range	Relative area under distribution	Median Probability	Johnston et al. (2012) Median Probability	Difference in Calibrated Ages
GX-30550	1046	3330+/- 70	3438 - 3719	0.946	3558	3565	7
GX-30549	1095	2890+/- 70	2847 - 3232	0.998	3029	3035	6
GX-30548	1158	4130+/- 90	4436 - 4842	0.991	4656	4658	2

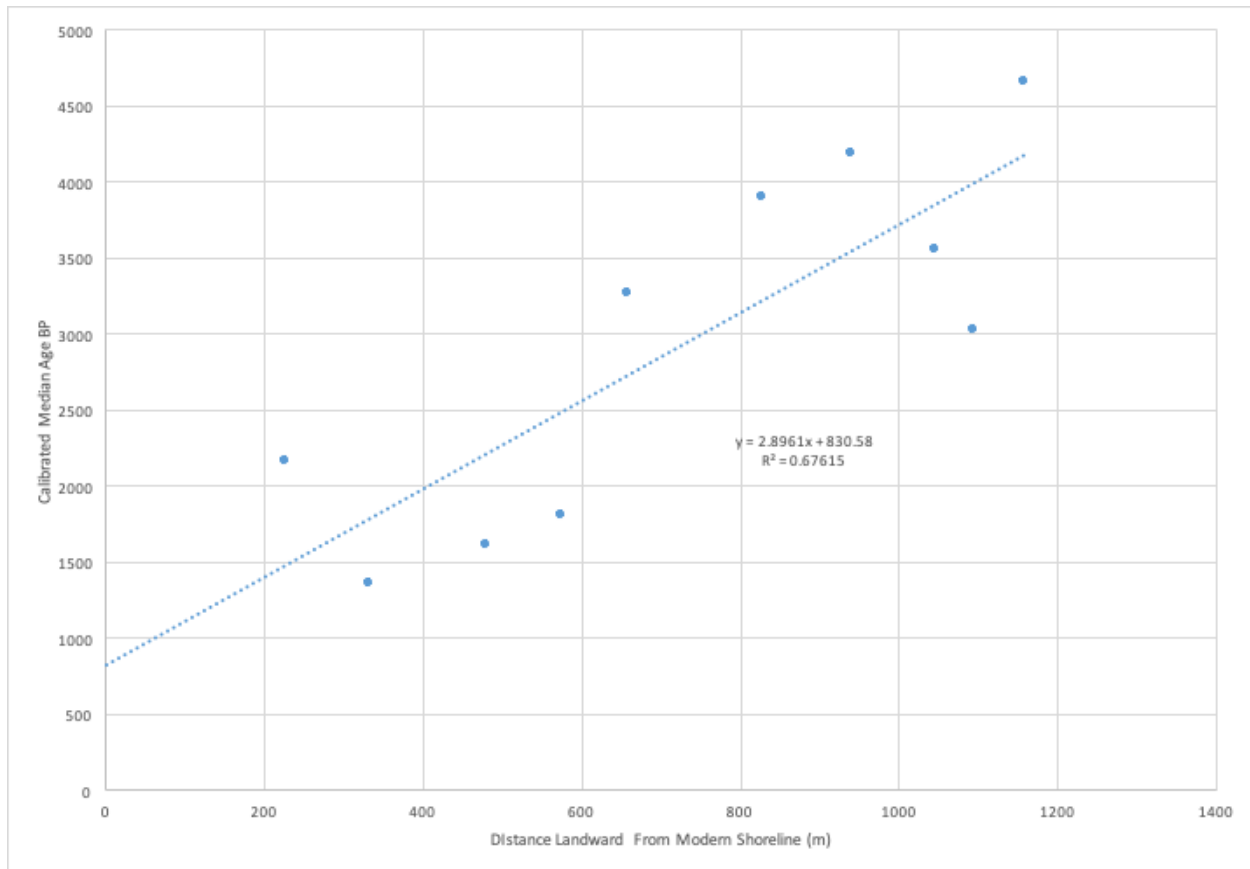


Figure 8. Calibrated radiocarbon ages of SSM beach ridges. Graphed versus their respective distance landward from the modern shoreline in the SSM strandplain. Linear age model showing a rate of change of approximately 2.9 meters per year.

As demonstrated in Figure 8 radiocarbon ages can be variable, but still generally follow the expected trend of getting younger as the ridges become more lakeward. In Johnston et al. (2012) this variability was also noticed and therefore OSL ages were collected, but OSL ages were not available for this project. The observed variability in radiocarbon can be caused by many factors that are beyond the scope of this thesis, and will not be discussed here. The ages observed in Figure 8 that do not follow the trend of being younger as the ridges move more lakeward could be variable due to the inaccuracy of the radiocarbon ages. Radiocarbon ages from basal wetland sediments found in swales are not direct measurements of the ridges where

cores were collected that best represent ancient lake levels. Radiocarbon ages reflect the age of their respective wetland instead which only forms sometime after the next lakeward adjacent ridge forms. So these wetlands could have also not immediately formed after the creation of their confining ridges and post depositional processes such as external water inputs from groundwater could alter the radiocarbon ages in wetlands. Both of these factors could cause the variability seen between the samples in Figure 8. The linear age model constructed for the SSM strandplain from radiocarbon ages of wetland sediments shows a slope of approximately 2.9 meters per year landward, which described an average progradation rate for the study site (Figure 8).

The age model constructed for the SSM strandplain in Figure 8 (Distance versus age) was used to calculate an age for every beach ridge, relative to distance from the modern shoreline. This was then applied to the distances in Figure 5 (distance versus elevation) to create a swale cross-strandplain elevation trend and FSB relative paleohydrograph with approximate ages on the horizontal axis and elevations on the vertical axis (Figure 9). To apply this age model, the distance landward that was measured at the location of each core on the lakeward side of the ridges was input as the x value in the age model in Figure 8 to obtain an approximate calendar year BP for every beach ridge in the SSM strandplain. The age of each ridge was then graphed versus their respective swale and FSB elevations. In Figure 9 the average difference between the field measured swale elevations and FSB elevations would still apply since the elevations were not changed by using the age model and the swale cross-strandplain elevation trend continues to show the same similarities to the FSB relative paleohydrograph. Figure 9 shows that the swale elevations would be suitable to use as a proxy for FSB elevations when the correction factor of 1.49m is applied, and the resulting cross-strandplain elevation trend could be used as a

representation of ancient lake levels when elevations are graphed versus time, resulting in an inferred paleohydrograph.

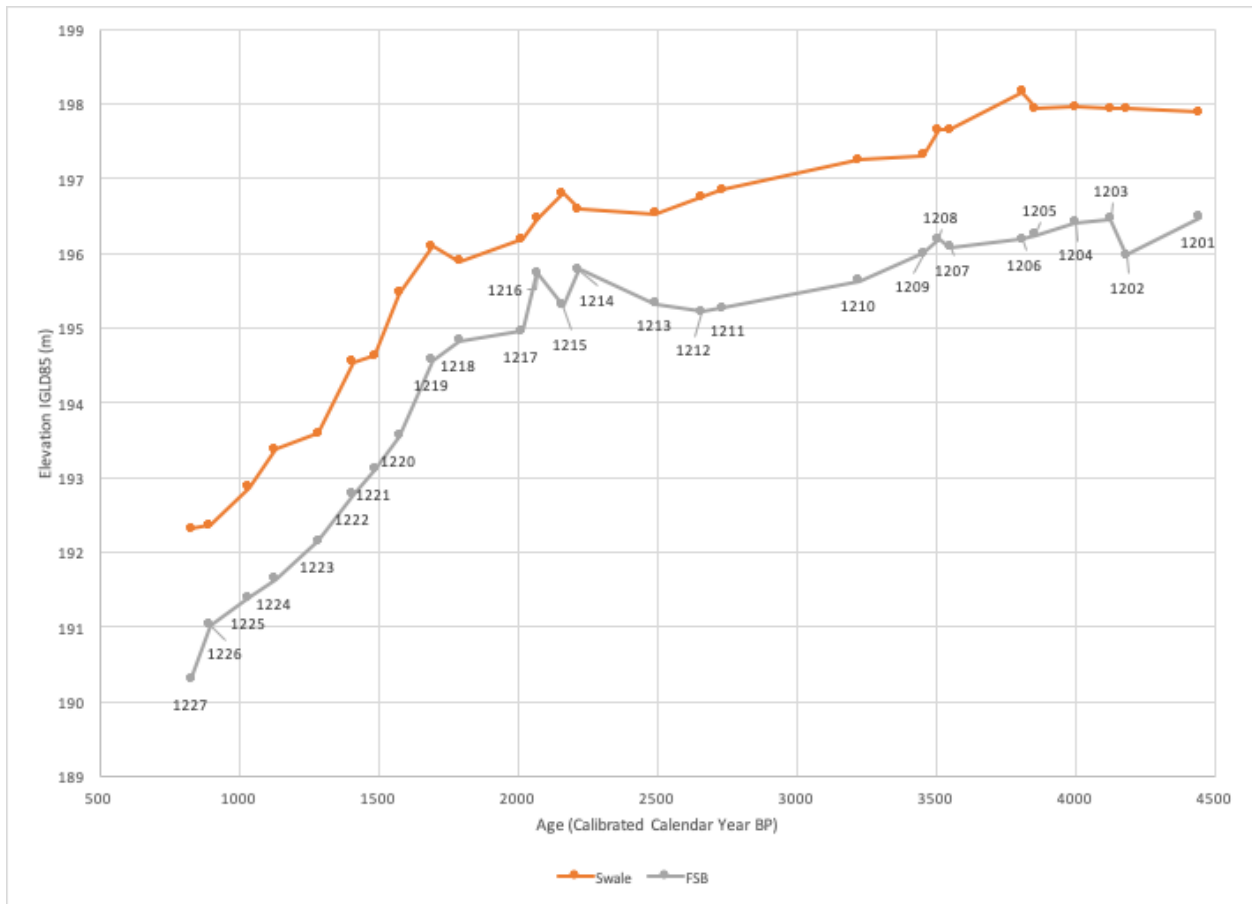


Figure 9. Field measured elevations versus age of ridges. Plot of age versus elevation data related to individual beach ridges in the SSM strandplain. An updated SSM paleohydrograph (FSB) from Johnston et al. (2012) with calibrated radiocarbon ages and a new age model.

LiDAR

Elevations of swales within the SSM strandplain were collected from LiDAR data to create a new cross-strandplain elevation trend. Swale elevations were collected from LiDAR data because in the field measured elevation data the swale elevations most closely matched the FSB elevations within the Nipissing phase at the SSM site. The topography of the SSM strandplain was obtained from a DEM raster (Figure 10) that was generated from the LiDAR ground points

of the SSM study site obtained from the NOAA digital coast (NOAA Digital Coast Data Access Viewer, 2021). A topographic profile that provides a cross sectional view of the SSM strandplain was constructed from a transect line that was created to be approximately perpendicular to the ridges that are seen on the DEM of the SSM strandplain (Figure 11). This transect was created to extend across the entire distance of the ridges in the SSM strandplain, and used the cores originally from Johnston et al. (2012) to interpolate the best location for the transect by attempting to follow the same path landward as the cores did while keeping the core locations equally distant from the transect.

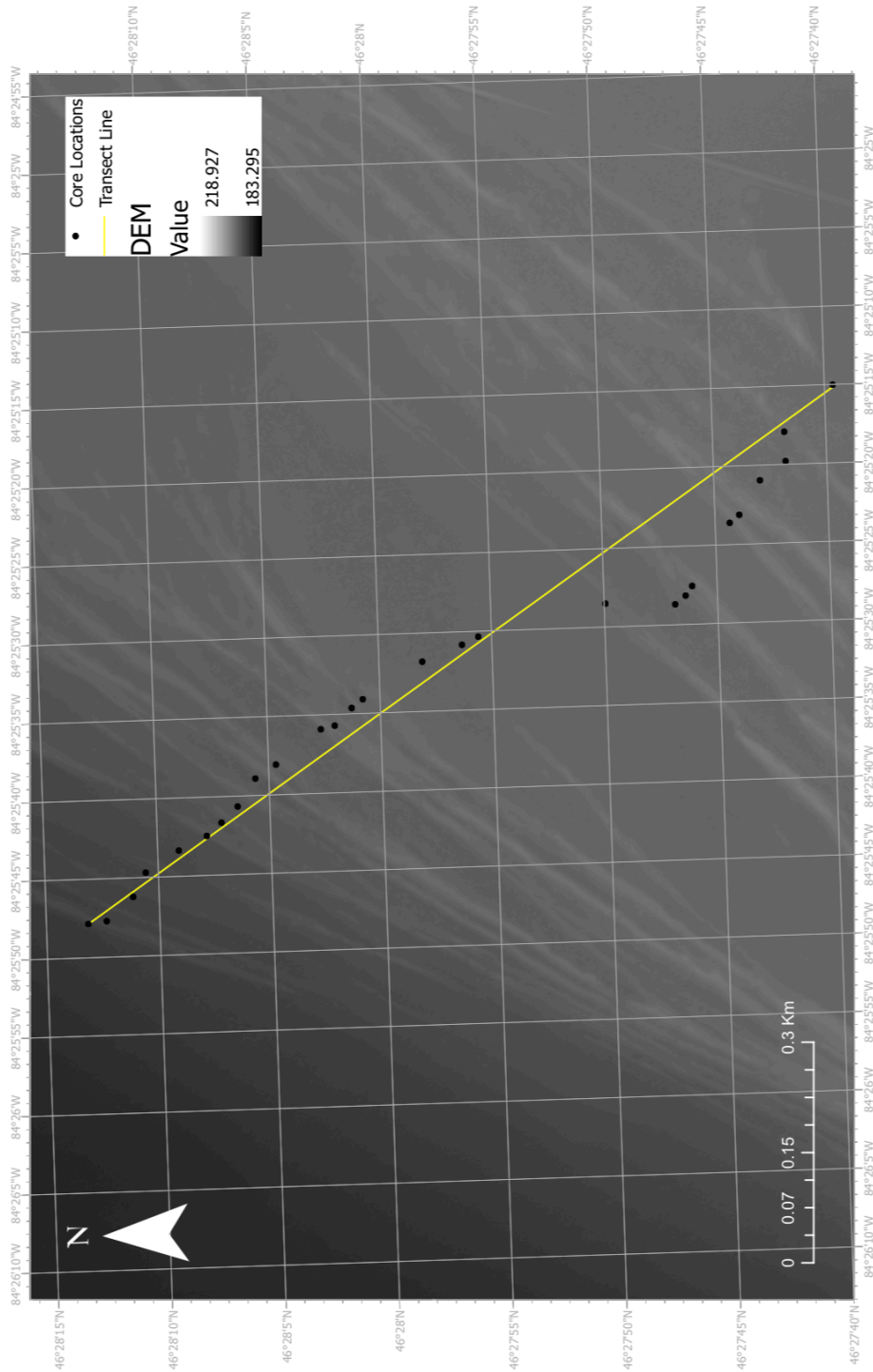


Figure 10. Sault Ste. Marie strandplain DEM. DEM map of the SSM strandplain shows the topography of the SSM strandplain and surrounding area. The locations of the cores in Johnston et al. (2012) and transect line used in this project are shown on the map.

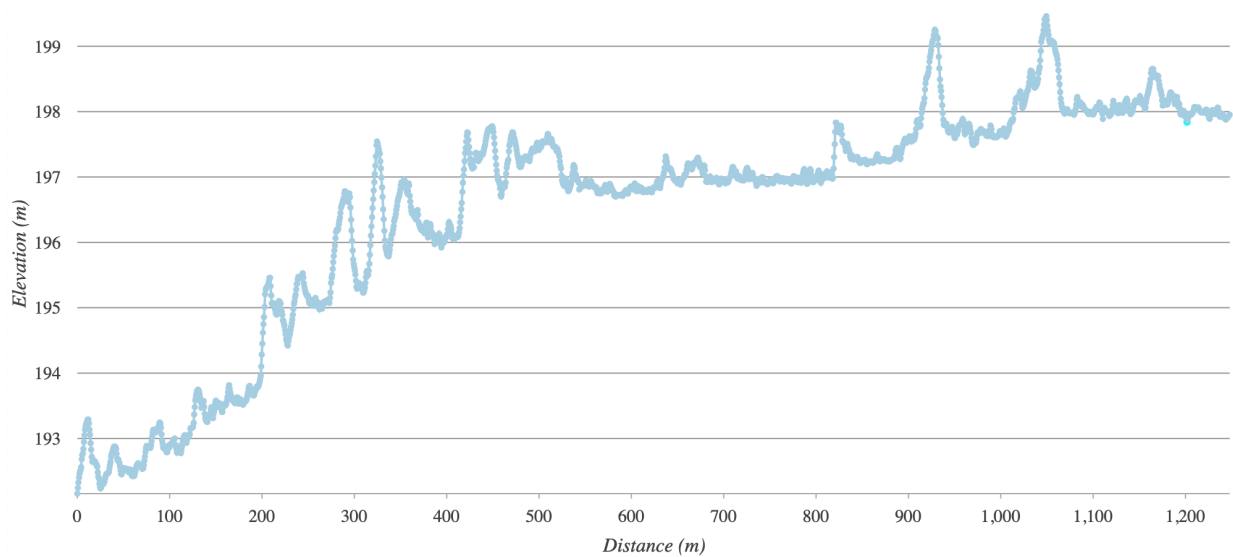


Figure 11. Sault Ste. Marie strandplain elevation profile. The topographic profile occurs along the transect line shown in Figure 10. The cross-strandplain topographic profile shows ridges as increases in elevation and swales occur between those ridges. From left to right the cross-strandplain topographic profile extends approximately in the north east to south west direction.

The cross sectional topographic profile derived from LiDAR data of the SSM strandplain in Figure 11 shows a trend similar to the cross-strandplain elevation trends seen in Figure 5 (swale cross-strandplain elevation trends and FSB relative paleohydrographs). The cross sectional topographic profile shows much greater variability between the elevations along its distance when compared to the cross-strandplain elevation trend of the field measured swale elevations and the FSB relative paleohydrograph in Figure 9. This is due to the large amount of elevation data points along its distance which record both swales and ridges. The high level of variation seen along the cross sectional topographic profile when compared to the FSB relative paleohydrograph is what prevents the topographic profile from being used in its entirety as a proxy for FSB elevations and ancient lake levels. To reduce the variation seen in the cross section and create a cross-strandplain elevation trend that is an appropriate proxy for FSB

elevations the elevations of the swales in the study site were collected using the procedure in the LiDAR section of the methods.

Swale elevations were collected from the cross-strandplain topographic profile in Figure 11 by using ArcGIS Pro and following the procedure laid out in the LiDAR subsection of the methods. The distance landward of each individual swale used to obtain elevations were converted to approximate calendar year BP by using the individual swales distance landward as the x value in the age model from Figure 8. The elevations of the individual swales and their corresponding approximate calendar year BP were then graphed to show a cross-strandplain elevation trend in Figure 12 and are represented by the blue markers and line.

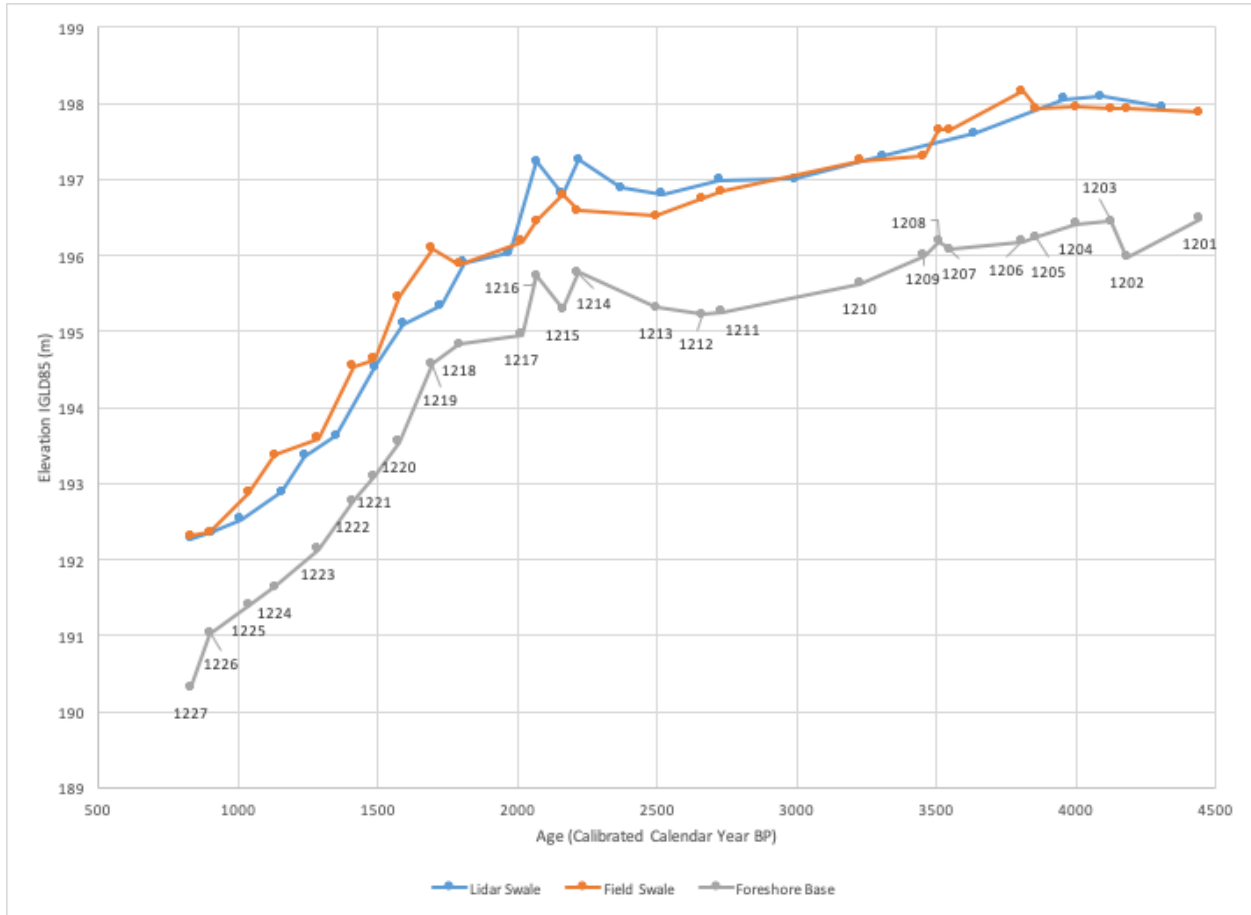


Figure 12. Paleohydrograph of the SSM strandplain including LiDAR swale elevations. LiDAR swale elevations create cross-strandplain elevation trend reconstructed from LiDAR swale elevations. The LiDAR swale cross-strandplain elevation trend shows a similar trend to both FSB and field swale trends. The LiDAR and field swale trends overlap in places and have similar elevation values across their distances.

The cross-strandplain elevation trend made from LiDAR swale elevations in Figure 12 shows a similar trend to those seen in the trends reconstructed from field swale elevations and FSB elevations. More detailed patterns seen in the field swale and FSB trends can also be seen in LiDAR swale cross-strandplain elevation trend. The minimum elevation value for the LiDAR swale cross-strandplain elevation trend is almost the same as the minimum in the field swale elevation trend at 192.27 m and 192.31 m respectively. The end points of the field and LiDAR

swale cross-strandplain elevation trends are also similar at 197.95 m and 197.88 m respectively. One area where there is a noticeable difference between the field and LiDAR swale elevation trends is between 2000 years BP and 2500 years BP. Between these ages the max of the LiDAR trend is 197.24 m while the field swale max elevation is 196.8 m. Figure 12 shows that, although there are differences between the field swale and LiDAR swale cross-strandplain elevation trends, they show a similar cross-strandplain trend. Due to this similarity between the LiDAR and field swale elevations, the LiDAR swale elevations can be used as a proxy for the FSB elevations and relative lake level when the correction factor of 1.49 m is applied.

The mean difference between the field swale elevations and the FSB elevations of 1.49 m in Table 2 was applied as a correction factor to the swale elevations obtained from LiDAR (Table 4). These corrected elevations were graphed versus calibrated age BP for the strandplain as an inferred paleohydrograph alongside the FSB relative paleohydrograph (Figure 13). Figure 13 shows that with the correction factor applied, the LiDAR swale inferred paleohydrograph is an accurate proxy for the ancient levels in the FSB relative paleohydrograph. Since LiDAR swale elevations are an accurate proxy for FSB elevations, the LiDAR swale elevations can be used to infer ancient lake levels and ancient lake-level trends recorded by relict shorelines at the SSM strandplain deposited during the Nipissing phase. Some variations can be seen between the two trends notably between 1500 and 2000 calendar years BP as well as 4000 and 4500 calendar years BP. Between these ages the LiDAR swale elevations show the greatest difference to the FSB elevations. The difference between the mean elevations of the inferred paleohydrograph and relative paleohydrograph is approximately 0.37 m.

Table 4. LiDAR swale elevation data. Includes IGLD85 datum adjustments done using National Geodetic Survey (NGS) Tool Kit online program IGLD85 Height Conversion (NGS, n.d.) Also includes elevations corrected with correction factor. Uses correction factor of -1.49 m.

Swale Number	Distance Landward (m)	Elevation NAVD88 (m)	Elevation IGLD85 (m)	Corrected Elevation IGLD85 (m)
1	0	192.16	192.27	190.78
2	25.2	192.24	192.35	190.86
3	61.2	192.42	192.53	191.04
4	112.19	192.78	192.89	191.4
5	140.39	193.25	193.36	191.87
6	179.39	193.52	193.63	192.14
7	227.98	194.42	194.53	193.04
8	262.18	194.98	195.09	193.6
9	309.58	195.23	195.34	193.85
10	337.17	195.79	195.9	194.41
11	394.17	195.92	196.03	194.54
12	427.77	197.13	197.24	195.75
13	458.97	196.7	196.81	195.32
14	479.36	197.15	197.26	195.77
15	531.56	196.78	196.89	195.4
16	582.56	196.7	196.81	195.32
17	653.35	196.88	196.99	195.5

Table 4. Continued.

Swale Number	Distance Landward (m)	Elevation NAVD88 (m)	Elevation IGLD85 (m)	Corrected Elevation IGLD85 (m)
18	747.54	196.89	197	195.51
19	855.53	197.2	197.31	195.82
21	970.13	197.49	197.6	196.11
23	1079.32	197.95	198.06	196.57
24	1126.71	197.98	198.094	196.604
25	1201.71	197.84	197.95	196.46

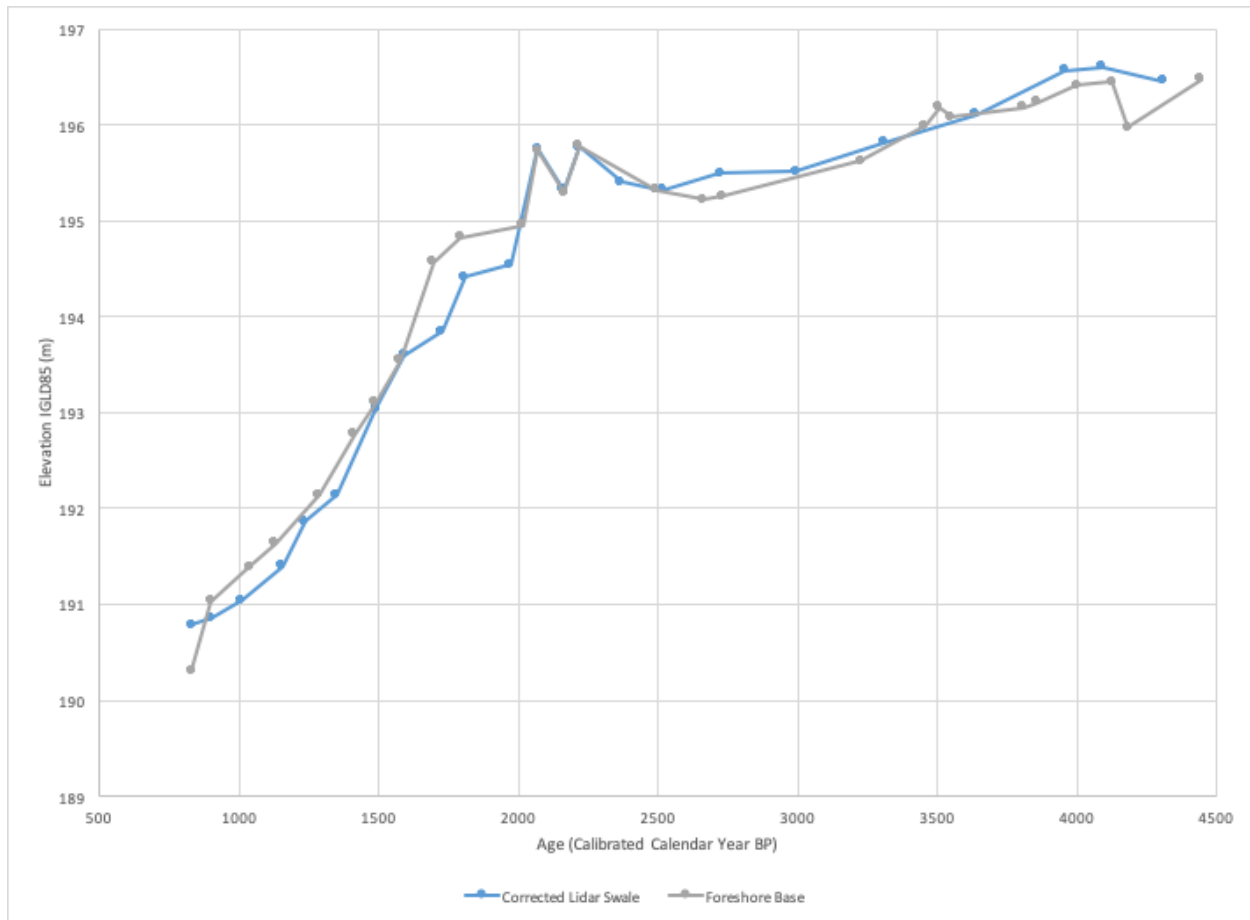


Figure 13. Inferred paleohydrograph for the SSM strandplain site. Relative lake-level trends reconstructed from the FSB elevations and corrected LiDAR swale elevations.

Discussion

Field Measured Elevation Data Analysis

Analyses of the SSM strandplain determined that the topographic elevation of the swales formed during the Nipissing phase in the SSM strandplain were the best topographic proxy for the FSB elevations. The consistent difference in elevation, with a small standard deviation and small range showed that the elevation of the swales within the SSM strandplain would be the best topographic proxy for the FSB. The ridge crest to FSB elevation differences had a standard deviation and range that were larger than the swale to FSB elevation differences, making the

ridge crest less representative of the FSB across the SSM strandplain. The cross-strandplain elevation trend of the ridge crests also had more points where the trend changed direction and was more variable than that of the swale (Figure 5). The results also showed that when there is a noticeable change in the trend of the FSB relative paleohydrograph, the swale cross-strandplain trend follows approximately the same path as the FSB relative paleohydrograph. By determining that the swale elevations were the best topographic proxy for the FSB elevations, and that they were consistently similar to the FSB relative paleohydrograph across the entire distance landward, a correction factor was established. This correction factor was the calculated mean difference between the swale topographic elevations and the FSB elevations. The final correction factor value for the SSM strandplain site was 1.49 m and was subtracted from the LiDAR swale elevations.

The results showing that the ridge crest elevations were variable and inconsistent when compared to the FSB were expected. The dune cap which contributes to many ridge crest elevation changes in strandplains are related to aeolian processes and not necessarily lacustrine processes. Erosion, transportation and deposition, of dune caps are dependent on many factors that include weather or specifically wind direction and velocity, vegetation and sediment. Elevation of dune caps on ridges can be unrelated to the ancient lake level and not the most accurate representation of the environmental conditions at the time of deposition (c.f. Tamura, 2012). The lacustrine sediment which forms the core of the ridge and the FSB is preserved inside ridges and considered “protected” from subsequent processes after the core of the ridge forms. Since the FSB sediments are buried, the lake level that resulted in their deposition is preserved. With the variation in elevation of the ridge crests created through aeolian processes and not lacustrine processes the elevations of the ridge crests are not the best predictors of ancient lake

levels. The multiple increases and decreases between individual ridge crest elevation points do not reflect the trends of water levels over time, and therefore would be misleading to interpret past lake-level trends and patterns. The observed elevation consistency of the swales could be partially due to the lacustrine and not aeolian nature of this sediment and not being covered or modified after the lake water initially formed the ridge.

Results in this thesis also found that the swale cross-strandplain elevation trend and FSB relative paleohydrograph were separated at a point of visible change in their cross-strandplain trends, the swale elevation trend followed a similar trend to the corresponding FSB cross-strandplain elevation trend (relative paleohydrograph) even though the two plots were consistently separated (Figure 7). A common cross-strandplain elevation trend was important in determining if the swale elevations would be appropriate to use as a proxy for the FSB because the change observed at 400 m in the FSB relative paleohydrograph is important and associated with high relative lake levels at SSM. This point of change in the cross-strandplain trends represents a point of change in the rate of lake level change, and to be an alternative for the FSB the swale elevations must follow the same trend as the FSB on both sides of the changing trend. If the swale elevations were found to not follow a similar trend on both sides of core 1218, two separate correction factors would be needed to adjust the swale elevation down to the FSB elevations, representing the relative elevation of ancient lake levels. Finding that the swale elevations are similar to the FSB elevations on both sides of the observed point of change showed that even with changes in lake-level trends swale elevations will still accurately reflect lake level when a single correction factor is applied. This result reinforces the finding that the swale elevations can be used as an alternative elevation to elevations derived from coring FSB in

ridges, representing ancient lake level elevations. This alternative approach provides new knowledge that the swale elevations follow FSB trends in the SSM strandplain.

Application of Topographic Elevation Data

In the literature review it was discussed that topographic methods previously applied to strandplain studies were inaccurate and variable. Reconstructing paleohydrographs for lake basins from Great Lakes strandplains with variable topographic methods would have resulted in paleohydrographs that were not an accurate representations of ancient lake levels. In Larsen (1994) the methods used topography along with various subsurface elevations and were inconsistent in the application of these elevations, which resulted in paleohydrographs that did not accurately reflect ancient lake levels and their associated trends. These paleohydrographs were not representative of ancient lake levels and their trends and patterns because the topography of a strandplain is not directly generated by the water in the lake but other processes that include aeolian processes. Lake levels do influence the formation of the strandplains and their associated topographic features, however the effects of other depositional and erosional processes that occurred after the ridges initially formed could alter the topography of the strandplain. Since topographic elevations of features within a strandplain are not directly associated with lake level and include deposition from additional process at the time of their formation, an elevation measurement could relate to aeolian deposition and erosion rather than lacustrine processes. The methods developed in Thompson (1992) resolved the issue of variable topographic methods and suggested the use of a direct representation of lake level by using the water-lain foreshore base contact elevation or FSB. The results of this thesis connect the variable topographic methods used in Larsen (1994) and the most accurate methods developed in Thompson (1992).

Comparing FSB elevations, directly deposited by ancient lake level with topographic swale elevations allowed for a detailed evaluation of the strengths and weaknesses of using topographic swale elevations to reflect ancient lake levels. Topographic elevations could not be used alone, with confidence, until a relationship was established that ensured topographic elevations could be an appropriate reflection of ancient lake levels at the SSM strandplain. This thesis showed that swale elevations can be used as an alternative measurement to infer ancient lake levels in the SSM strandplain.

A correction factor was needed to adjust indirect topographic measurements down to inferred elevations that better represented ancient lake level elevations. The correction factor was calculated by using the relationship between the FSB elevations and the swale elevations across the entire SSM strandplain. The correction factor vertically brings down each of the individual swale elevations, on average to the FSB, and therefore to a better inferred ancient lake level elevation. Since the correction factor adjusts the swale elevations down to an estimated water-lain FSB contact elevation it helps interpret ancient lake levels when coring data is not available. However, the correction is applied as one factor to all swale elevations and not individually unique values in this study. It is recommended that in future studies correction factors for smaller groupings of ridges, as shown in cross-strandplain geomorphic and sedimentologic trends (Johnston et al. 2007) are explored to improve estimates of past lake level when correcting topographic swale elevations. Once the swale elevations are corrected they can be used to infer ancient lake levels and thus creates an alternative method for the reconstruction of an inferred paleohydrograph at the SSM strandplain.

Although this thesis provides a consistent way to use topographic elevations as an alternative method to create an inferred paleohydrograph for the SSM strandplain, there are

limitations. Researchers had to visit the SSM strandplain and measure topographic elevations (crest and swale point elevations) using survey equipment. This took funds and time to complete. The topographic and subsurface elevations (from cores) that were analyzed in this project were only from the SSM strandplain deposited during the Nipissing phase. Therefore, the alternative approach is only applicable to the SSM strandplain deposited in the Nipissing phase. These methods potentially could be applied to other strandplains that were deposited during the Nipissing phase but the 1.49 m average correction factor may not be appropriate for other strandplain locations. Other time periods need to be investigated as well. This thesis forms the basis to continue investigating the connection between strandplains topography as an alternative to FSB elevations at sites with no previous coring done.

LiDAR

A cross sectional topographic profile of the SSM strandplain was obtained by creating a transect along the entire length of the strandplain on a DEM created from LiDAR ground points. The topographic elevation cross section showed a high level of variability in elevation along its length, and would not have been appropriate to use as a proxy to infer ancient lake levels for the SSM strandplain. The variability in elevation of the topographic cross section was the result of it representing the entire strandplains topography, including both ridge crests and swales. The elevations of each individual swale within the SSM strandplain were extracted from the topographic cross section so that the LiDAR data could be better applied in the reconstruction of an inferred paleohydrograph. Swale elevations were then graphed versus their approximate age obtained from the age model, the single correction factor of 1.49 m was applied to the swale elevations in this graph. The resulting corrected swale topography cross-strandplain elevation trend was similar to the FSB relative paleohydrograph and thus the method used to reconstruct it

can be used as an alternative to reconstruct a paleohydrograph for a strandplain in the form of an inferred paleohydrograph for the SSM strandplain during the Nipissing phase.

LiDAR is a highly accurate way to remotely obtain ground elevations. Due to this high level of accuracy the cross sectional topographic view of the SSM strandplain was variable in elevation and showed changes in elevation that would not normally be observed and recorded in the field. These small changes in elevation appeared on Figure 11 (cross sectional topographic profile) and could be misinterpreted as ridges in the SSM strandplain. If LiDAR was being used at a strandplain without previous cores, these small changes in elevation could cause a misinterpretation of how many beach ridges are in the strandplain. By misinterpreting the number of beach ridges in a strandplain, the swale elevations that are collected could potentially not be representative of actual swales in the strandplain, and could therefore result in the reconstruction of a paleohydrograph that is not representative of inferred ancient lake levels. To avoid this problem at the SSM strandplain, and to create a method that could work for a site without previous cores the swales were identified and then extracted from the cross section. It is recommended that the use of air photos in identifying swales at a study site is explored to provide another method of obtaining the locations of swales on a cross-sectional topographic profile. Swales were chosen to be identified because the in-field elevations showed that swale elevations were the best topographic proxy for FSB elevations.

To identify the swales in the SSM strandplain, the ridges were first identified on the DEM, then the distance landward of those ridges along the transect was transferred onto the corresponding topographic cross section. The swales were then considered as the lowest points between those ridges, and in some cases with long swale sections between ridges it was the lowest point closest to the half way point. After identifying the individual points where there

were swales, the points respective elevation and distance landward was recorded and used to create a cross-strandplain elevation trend. This method was successful in reducing the variation seen in the topographic cross section by providing a way to reduce the need for inferring what was a beach ridge and what was a slight change in ground surface that the LiDAR ground points resolved. Using this method makes the application of LiDAR more reliable by reducing the chances of using an elevation that is not actually a swale and therefore not reflective of ancient lake levels.

One area that posed a challenge when extracting the swale elevation data from the cross sectional topographic profile was the selection of a distance landward to use for the elevations. In figure 5 (in-field cross-strandplain topographic profiles) all of the field measured elevations had the same distance landward and that distance was in respect to each ridges crest. The age model for the strandplain was also in respect to the distance landward of the ridges, so it would be preferable if the LiDAR swale elevations were also measured with distance landward to ridges. This would allow the distance landward to correspond to the FSB distance landward and thus make a more accurate inferred paleohydrograph. When the distance landward of the ridges on the cross-strandplain topographic profile were used for the swale elevations it created an inferred paleohydrograph that was much less accurate than the one in figure 13. This inaccuracy could have been caused by the variability seen in the ridge crests. As discussed previously, the ridge crests are subject to erosion, transportation and deposition processes unrelated to ancient lake level. These processes unrelated to lake level could potentially affect the distance landward of ridges creating variability between the ridges with no consistent distance between them. This could have affected the accuracy of the attempted inferred paleohydrograph with ridge crests as distance landward. To keep the methods of reconstructing and inferred paleohydrograph simple,

the distance landward of the elevation point used to measure the swale was used as its distance landward when graphing the cross-strandplain elevation trend and also in the age model. It is recommended that a method to relate the swales elevation to the ridge crest should be explored in the future. This would allow the swale elevation to directly overlie the FSB and thus create a more accurate inferred paleohydrograph.

Creating a topographic cross section in an appropriate location of the strandplain may be difficult without previous cores to base the creation of the transect off of. It is essential to create a transect that best represents the topography of the strandplain to properly interpret its topography with LiDAR elevation data. The first aspect of the cross section to consider is that it needs to be perpendicular to the ridges. By making the transect for the topographic cross section perpendicular, the distances between ridges will be the best representation of the movement of the margins of the water and thus lake level. The transect should also cover every ridge that needs to be studied, if it appears that there are more ridges within the distance landward of focus in one area over another those ridges should be included in the transect to ensure an accurate representation of ancient lake level. The transect should be created where the ridges have the greatest distance between them. This would allow easier resolution of individual ridges and swales easier by maximizing the distance between them and thus making the changes in topographic elevation more evident on the cross sectional topographic profile. This means sections like the south west of SSM where the ridges are close together would not be appropriate for a transect. Further research should be done into this factor of using LiDAR to ensure that transects are providing accurate representation of the strandplain sites being studied.

Ages

The ages used in this project were radiocarbon ages of sediment samples collected from the bottom of wetlands in Johnston et al. (2012) that occur in the swales of the SSM strandplain. The use of these wetland samples for ages is based off of the assumption that the wetlands formed immediately after the formation of the confining ridges. This assumption may not be correct for the wetlands. It was found that multiple ages of samples that did not follow the expected trend of the ridges getting younger as they become more lakeward. These ages of these wetland samples could have been altered from external factors, or the formation of the wetlands may have not followed the assumption that they formed immediately after the confining ridges. The use of OSL ages has been determined to be more accurate than radiocarbon since the sediments being dated are directly from the foreshore and are therefore directly related to the water level (Argyilan et al., 2005). To create a more accurate age model for future applications of this projects methods the use of a site with OSL ages of the ridges is recommended.

A limitation of the methods presented in this project involves the need for age data to reconstruct paleohydrographs. LiDAR data provides highly accurate spatial data that can be used to remotely find elevation and distance landward that can be used in the reconstruction of paleohydrographs. However, to reconstruct a paleohydrograph the ages of the ridges and an age model for the strandplain study site are required. There is no remote way to obtain age data, so these methods would still require the collection of sediment samples to obtain the ages of the ridges at the study site and to develop an appropriate age model for the study site.

Implications

This thesis showed that LiDAR swale elevations along with an appropriate correction factor can be used as an alternative to FSB elevations to reflect ancient lake levels when

reconstructing paleohydrographs. The use of LiDAR to reconstruct inferred paleohydrographs creates the opportunity to study strandplains that are difficult to access for field work and core. This new method uses a remote method by analyzing LiDAR to estimate the elevation of past lake levels in ancient shorelines. Analysis of more strandplain sites across the Great Lakes can help refine the spatial and temporal understanding of ancient lake levels, providing insight into natural trends and patterns of ancient lake levels impacted by climate, GIA and changes in active outlets. The use of LiDAR could help fill in gaps of time that have not been studied yet providing a more comprehensive understanding of ancient lake levels. This method could also be applied to new strandplain sites in different locations around the lake basins to help study the effects of GIA to relative lake level. A major application of the new method presented in this thesis would also be in the preparation aspect before for field work is conducted. Reconstructing paleohydrographs from LiDAR topography can help gain insight into a new site before completing field work. The results from this could help guide the field work and potentially alter plans before field work has begun. For example, the inferred paleohydrograph could help identify areas in the strandplain with the most number of beach ridges and reveal potential core locations to obtain FSB elevations. This could also help select potential sampling areas for age analysis like OSL age-dating. LiDAR data is the most detailed method to obtain topographic elevations and has provided a pathway for remote spatial analysis unlike anything previous. And much of this LiDAR data is free to obtain especially along the U.S.A coastline of the Great Lakes, as the Canadian coastline is being collected. This allows for an inferred paleohydrograph to be reconstructed in an inexpensive manner which can help reduce costs of field work by guiding the process and making the researches better prepared for field work. One such preliminary application is in Opersko (2021) where a fellow undergraduate student applied this

method to strandplain data in the Stockton Island Tombolo (SIT), Apostle Island National Park, Wisconsin, U.S.A. Opersko's (2021) inferred paleohydrograph for SIT is helping guide field work and will be evaluated after field work has been completed. The new methods presented in this thesis has incredible potential but should really be investigated in different strandplains and different parts of the strandplain that were deposited in time periods other than the Nipissing phase.

Conclusion

The Great Lakes are currently experiencing high water levels, which are negatively impacting stakeholders, coastal infrastructure, and coastal environments. Understanding the context for the high lake levels that are being experienced today, and past natural lake-level fluctuations is essential in mitigation their impacts and preparation efforts. To understand lake-level fluctuations stakeholders normally examine the historical or instrumental records of lake level to gain insight into past trends and patterns that could be projected into the future. But it is also essential to understand the long-term or natural fluctuations of ancient lake-level trends and patterns that provide context for modern changes in lake levels. Ancient natural lake-level trends and patterns are derived from strandplains of beach ridges that have within them a preserved record of ancient lake levels, providing a valuable source of detailed information about natural conditions.

Summarized in Johnston et al. (2014), they describe that Baedke and Thompson (2000) in the Michigan basin and Johnston et al. (2012) in the Lake Superior basin have applied the subsurface coring method developed in Thompson (1992) to study strandplains and reconstruct the most detailed account of ancient lake-level trends and patterns in paleohydrographs. This thesis provides a potential alternative method, where coring individual beach ridges has not been

completed yet or is not feasible to preliminarily infer the elevation of ancient lake levels recorded in strandplains. The potential to reduce costs and increase the accessibility of studying relict shorelines of the Great Lakes strandplains creates an opportunity to apply this alternative method in many future studies. This alternative method could expand insight into ancient lake-level trends and patterns by bridging gaps of time that have not been studied, and by studying new strandplains that have previously had no field completed. By expanding insight into ancient lake-level trends and patterns stakeholders can gain more detailed and refined context for current high levels, historical fluctuations and the underlying natural geological fluctuations. In doing this, stakeholders can then gain new perspectives and better context to the relatively high lake levels causing erosion and flooding and can better prepare for potential future fluctuations in lake levels of the Great Lakes.

Recommendations

The results of this thesis are limited to only the SSM strandplain within the Nipissing phase, and therefore it is recommended that the methods of this thesis should be expanded to new locations with strandplains and lake level phases within the Great Lakes (i.e. Algoma, Sault, Sub-Sault described in Johnston et al. 2014). The methods used in this project should first be applied to additional strandplain sites within Lake Superior that have previously had field work completed for them to determine if the elevations of the swales within the strandplains are consistently the best proxy for the FSB elevations. This can be done by applying the same statistical tests to the strandplain sites being studied, and by reconstructing cross-strandplain elevation trends, relative paleohydrographs and inferred paleohydrographs to visually analyze for similarities. If it is determined that the topographic elevation of the swales at different strandplain sites are also the best proxy for the respective strandplains FSB elevations a

correction factor should be established for those individual strandplains. The correction factors for the new sites should then be compared to determine if there are any similarities between them, by determining similarities a basin-wide correction factor could potentially be established. This basin-wide correction factor could potentially represent all strandplains within the Lake Superior basin and be used to correct swale elevations to be representative of ancient lake levels at sites that have previously not had field work done on them. However, one correction factor may not be appropriate for an entire basin or even within a single strandplain. The cross-strandplain trend of FSB elevations could change relative to swale elevations across a strandplain and therefore require multiple correction factors. This should be explored further to see if multiple correction factors could be used within a strandplain for groups of ridges to reconstruct a more accurate inferred paleohydrograph. The relation of individual swales distant landwards to their corresponding ridge crests distance landward should also be explored to determine if the ridge crest distance landward can be applied to swale elevations when graphed and in age models.

If there is an appropriate basin-wide correction factor for Lake Superior, or any other Great Lake basins, it should be attempted to try to apply the correction factor to a strandplain site that has not previous had field work completed. To do this field work would have to be done to collect the ages of the ridges at the site to reconstruct an inferred paleohydrograph. The elevations should be obtained from LiDAR and then graphed versus the ridges approximate age in calendar years BP. The resulting inferred paleohydrograph should then be compared to other paleohydrographs that have been reconstructed from other sites. By comparing the new inferred paleohydrograph to existing ones reconstructed from FSB elevations it can be determined if the LiDAR swale elevations created an appropriate inferred paleohydrograph. If it is found the

LiDAR swale elevations are an appropriate alternative to FSB elevations in the reconstructions at sites with no previous field work completed this method could be used in future applications to expand the understanding of the Great Lakes ancient lake-level trends and patterns.

References

- Argyilan, E. P., Forman, S. L., Johnston, J. W., & Wilcox, D. A. (2005). Optically stimulated luminescence dating of late Holocene raised strandplain sequences adjacent to lakes Michigan and superior, upper peninsula, Michigan, USA *Quaternary Research; Quat.Res*, 63(2) 122–135. doi: 10.1016/j.yqres.2004.12.001
- Baedke, J. S., & Thompson, A. T. (2000). A 4,700-year record of lake-level and isostasy for lake Michigan. *Journal of Great Lakes Research*, 26(4), 416-426. doi:10.1016/S0380-1330(00)70705-2
- Coordinating Committee on Great Lakes Basic Hydraulic and Hydrologic Data. 1995. Establishment of International Great Lakes Datum (1985). Coordinating Committee on Great Lakes Basic Hydraulic and Hydrologic Data, Chicago, Ill., and Cornwall, Ont.
- Fuller, K., Shear, H., & Wittig, J. (1995). *The great lakes: An environmental atlas and resource book* (3rd ed.). Toronto: Govt. of Canada.
- Gronewold, A. D., Fortin, V., Lofgren, B., Clites, A., Stow, C. A., & Quinn, F. (2013). Coasts, water levels, and climate change: A great lakes perspective. *Climatic Change*, 120(4), 697-711. doi:10.1007/s10584-013-0840-2
- Gronewold, A. D., & Rood, R. B. (2019). Recent water level changes across earth's largest lake system and implications for future variability. *Journal of Great Lakes Research*, 45(1), 1-3. doi: 10.1016/j.jglr.2018.10.012
- Hartmann, H. C. (1990). Climate change impacts on Laurentian Great Lakes levels. *Climatic Change*, 17(1), 49-67. doi:10.1007/BF00149000

International Joint Commission. (n.d.). Great lakes - St. Lawrence river basin. Retrieved from <https://www.ijc.org/en/great-lakes-st-lawrence-river>

Johnston, J. W., Argyilan, E. P., Thompson, T. A., Baedke, S. J., Lepper, K., Wilcox, D. A., & Forman, S. L. (2012). A sault-outlet-referenced mid- to late-Holocene paleohydrograph for lake Superior constructed from strandplains of beach ridges. *Canadian Journal of Earth Sciences*, 49(11), 1263-1279. doi:10.1139/e2012-057

Johnston, J. W., Thompson, T. A., & Baedke, S. J. (2007). Systematic pattern of beach-ridge development and preservation: Conceptual model and evidence from ground penetrating radar. *Geological Society of America Special Papers*, 432, 47. doi:10.1130/2007.2432(04)

Johnston, J. W., Thompson, T. A., & Wilcox, D. A. (2014). Palaeohydrographic reconstructions from strandplains of beach ridges in the laurentian Great Lakes. *Geological Society Special Publication*, 388(1), 213-228. doi:10.1144/SP388.22

Larsen, C. E. (1994). Beach ridges as monitors of isostatic uplift in the upper great lakes. *Journal of Great Lakes Research*, 20(1), 108-134. doi:10.1016/S0380-1330(94)71135-7

Millerd, F., (2011). The potential impact of climate change on great lakes international shipping. *Climatic Change*, 104(3), 629-652. doi:10.1007/s10584-010-9872-z

National Geodetic Survey. (n.d.). IGLD 85 height conversion [computer software] at <https://geodesy.noaa.gov/cgi-bin/IGLD85/IGLD85.prl>, accessed 2021-4-7

- National Oceanic and Atmospheric Administration (NOAA) Coastal Services Center.
(2012). *LIDAR 101: An introduction to LIDAR technology, data, and applications*.
Charleston, SC: NOAA Coastal Services Center. Retrieved
from <https://coast.noaa.gov/data/digitalcoast/pdf/LIDAR-101.pdf>
- National Oceanic and Atmospheric Administration (NOAA) Digital Coast Data Access Viewer.
Custom processing of "2016 - 2017 NRCS LiDAR: 30 County MI". Charleston, SC: NOAA
Office for Coastal Management. Accessed Feb 15, 2021 at
<https://coast.noaa.gov/dataviewer>.
- Opersko, D. (2021). *Remote paleohydrograph reconstruction for the stockton island tombolo*.
(Undergraduate thesis, University of Waterloo, Waterloo, Canada)
- Otvos, E. G. (2000). Beach ridges — definitions and significance. *Geomorphology (Amsterdam, Netherlands)*, 32(1-2), 83-108. doi:10.1016/s0169-555x(99)00075-6
- Rau, E., Vaccaro, L., Riseng, C., & Read, J. G. (2020). *The dynamic great lakes economy employment trends from 2009 to 2018*. Retrieved
from <https://www.michiganseagrant.org/wp-content/uploads/2020/10/MICHU-20-203-Great-Lakes-Jobs-Report.pdf>
- Sallenger, J., A.H., Krabill, W. B., Swift, R. N., Brock, J., List, J., Hansen, M., Stockdon, H.
(2003). Evaluation of airborne topographic LIDAR for quantifying beach changes. *Journal of Coastal Research*, 19(1), 125-133.
- Stuiver, M., Reimer, P.J., and Reimer, R.W., 2021, CALIB 8.2 [WWW program] at
<http://calib.org>, accessed 2021-4-7

- Tamura, T. (2012). Beach ridges and prograded beach deposits as palaeoenvironment records. *Earth-Science Reviews*, 114(3-4), 279-297. doi:10.1016/j.earscirev.2012.06.004
- Thompson, T. A. (1992). Beach-ridge development and lake-level variation in southern lake Michigan. *Sedimentary Geology*, 80(3), 305-318. doi:10.1016/0037-0738(92)90048-V
- Thompson, T. A., & Baedke, S. J. (1997). Strand-plain evidence for late Holocene lake-level variations in lake Michigan. *Geological Society of America Bulletin*, 109(6), 666-682. doi:10.1130/0016-7606(1997)109<0666:SPEFLH>2.3.CO;2
- USACE. (2020). Great lakes hydraulics and hydrology. Retrieved from <https://www.lre.usace.army.mil/Missions/Great-Lakes-Information/Great-Lakes-Information-2/Water-Level-Data/>
- Wilcox, D., Thompson, T., Booth, R., & Nicholas, J. R. (2007). Lake-level variability and water availability in the great lakes. *U.S. Geological Survey Circular 1311*

Appendix A: Thesis Design Poster

Comparing Paleohydrograph Reconstructions from Subsurface Stratigraphy and Topography

Marcel Heather, Supervisor: John Johnston




Figure 1: Map of the Great Lakes Drainage Basin. Sub-drainages are color-coded: blue for the western basin, green for the central basin, and red for the eastern basin. Water levels are indicated by different shades of blue. The map shows the extent of the basin and the locations of various sub-drainages.

Introduction:

- The Great Lakes water shed is home to more than 30 million people in Canada and the United States. This transboundary watershed supports a vital environment, society and economy. Size of basin shown in Figure 1 (US EPA, 2015).
- Changes in land use, climate, and water management have led to changes in water levels and basin health (Rise et al., 2020).
- We are currently near record high water levels in the Great Lakes as seen in Figure 2 (Greenwood and Hood, 2019).
- Streamflow infrastructure
 - Crestal erosion and flooding
 - Water level recorded since mid 1900s (Greenwood et al., 2013)
 - Changes in streamflow impact the residents and stakeholders
- Geologic lake levels have been reconstructed from subsurface stratigraphic contacts and ancient shorelines (Thompson, 1982; Beaulieu and Thompson, 2000; Johnston et al., 2012).
- Studied beach-ridges in Great Lakes embayments which create shorelines, examples of shorelines seen in Figure 3
- Reconstructed paleohydrograph by obtaining an elevation and age from an individual ancient shorelines
 - Reveal multi decadal to millennial trends and patterns of natural water level fluctuations
- Can topographic elevations be used to reconstruct paleohydrographs?
 - Potential method for areas that have not been visited or visited, needs a natural geologic trends and patterns used can provide context to understand modern water levels and may help create realistic scenarios for stakeholders to plan for future potential natural and anthropogenic trends

Objective:

- The objective of this project is to compare paleohydrograph reconstructions from subsurface stratigraphy to topography at Great Lakes embayments. This project aims to provide a new perspective on subsurface stratigraphic paleohydrographs and will develop recommendations for the use of the topographic method.

Goals:

- Reconstruct a paleohydrograph from topography
 - Connect the paleohydrograph to be as close to subsurface contact method
- Develop guidelines to apply topographic method
 - Identify areas where topographic method is most appropriate
 - Identify areas where topographic method is not appropriate

Literature Summary:

Variable approaches:

- Many methods have been used to reconstruct past lake levels
- Relationship between what was measured and interpreted as lake level was not consistent or accurate
- Methods of reconstruction of beach ridges, Lajtha (1984) for example collected sediments not directly related to lake level

A new consistent approach:

- Developed in Thompson (1982)
- Used specific subsurface stratigraphic contacts directly deposited at lake level, examples of basal beachline contact in Figure 5
- Basal beachline contact used to reconstruct ancient water level

Applying subsurface method:

- Thompson's (2000) method was applied at multiple stratigraphic sites in Great Lakes
- Lake Michigan (Thompson and Beaulieu, 1997 and Beaulieu and Thompson, 2000) and Lake Superior (Johnston et al., 2012)
- This method, using the subsurface stratigraphic contact to interpret ancient lake level is accepted to be the most accurate to reconstruct ancient water levels

Topographic:

- Newer topographic method of interpreting ancient water elevations to reconstruct paleohydrographs
- Investigate one recent application (Johnston et al., 2012) that briefly used the surface contact method along with topographic elevations
 - One correction factor was applied to topographic data to create one short paleohydrograph
 - Small correction factor based between the two types of paleohydrographs
- Early accessible data, LGEM being the most accurate for many stratigraphic sites
- Potential to create paleohydrographs from topography to compare with subsurface stratigraphic paleohydrographs

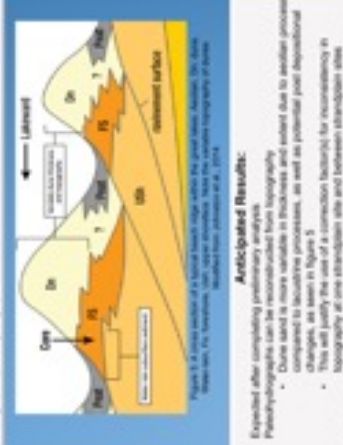


Figure 3: A cross-section of a lake basin showing topographic features and paleohydrograph reconstruction. The diagram illustrates the relationship between topographic elevation and paleohydrograph reconstruction. Key features include the lake level, beach ridges, and the paleohydrograph reconstruction. The diagram shows how topographic data is used to reconstruct the paleohydrograph, with a correction factor applied to the topographic data to create one short paleohydrograph.

Methods:

- To reconstruct a paleohydrograph an elevation and age for each beach ridge is required
- Light detection and ranging (LiDAR)
 - Flare units beams of light and calculates ranges based on return time of reflections (NOAA, 2012)
 - LiDAR is used to create a digital elevation model (DEM)
 - Vertical resolution of up to 10cm can resolve beach ridges (Schnager et al., 2000)
- Collect elevations
 - Water-lain subsurface stratigraphic contact (Beaulieu and Thompson, 2000 and Johnston et al., 2012)
 - Connect topography from LGEM to reflect lake level derived from water-lain stratigraphic contact
 - Collect ages obtained through dating of sediments directly around contact using optically stimulated luminescence (O.S.L.) Johnston et al., 2012)
 - Analyze elevation and age across multiple beach ridges at one stratigraphic site and between stratigraphic sites, inconsistencies will be established
 - Correction factor will be used to accurately represent lake level?
 - Figure 4 demonstrate flow of methods

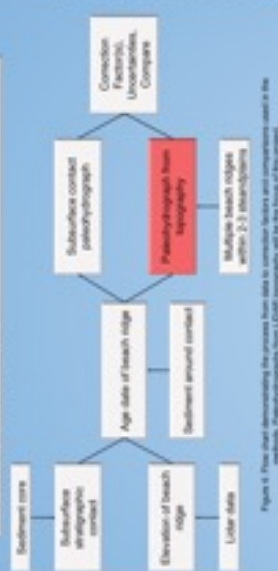


Figure 4: Flowchart illustrating the methodology for paleohydrograph reconstruction. The process starts with 'Subsurface stratigraphic contact' and 'Elevation of beach ridge'. These lead to 'Age date of beach ridge' and 'Subsurface contact paleohydrograph'. The 'Age date of beach ridge' leads to 'Paleohydrograph from topography'. The 'Subsurface contact paleohydrograph' and 'Paleohydrograph from topography' are compared to determine 'Connection Factors, Uncertainties, Compare'. This leads to 'Multiple beach ridges within 2-3 kilometers'. The 'Age date of beach ridge' also leads to 'Bediment around contact'. The 'Elevation of beach ridge' leads to 'Lider data'.

Anticipated Results:

- Expected after completing preliminary analysis
- Paleohydrographs can be reconstructed from topography
 - Done said is more variable in thickness and extent due to variable processes, compared to baseline processes, as well as potential post depositional changes, as seen in Figure 5
 - This will justify the use of a correction factor for inconsistency in topography and will be similar to subsurface stratigraphic paleohydrograph
- Lake level trends and patterns will be visible in paleohydrographs reconstructed using topography and will be similar to subsurface stratigraphic paleohydrograph
- This research will help provide context for modern high lake levels and develop a new method to reconstruct past lake levels that will allow for flexible investigation of sites that have not had field work completed

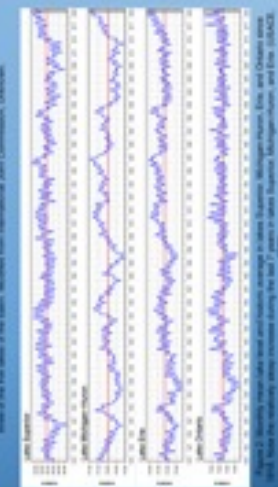


Figure 5: Four line graphs showing paleohydrograph reconstructions for different Great Lakes embayments: Lake Superior, Lake Michigan, Lake Huron, and Lake Erie. Each graph plots water level (m) over time (years). The graphs show the reconstructed paleohydrograph (blue line) and the subsurface stratigraphic paleohydrograph (red line). The graphs illustrate the variability in thickness and extent of the paleohydrographs reconstructed from topography compared to the subsurface stratigraphic paleohydrographs.

Conclusion:

- Topographic data can be used to reconstruct paleohydrographs
- Topographic data can provide context to understand modern water levels and may help create realistic scenarios for stakeholders to plan for future potential natural and anthropogenic trends

Figure 6: This chart demonstrates the accuracy from data to compare factors and consistency used in the methods. Paleohydrographs from LGEM topography will be the focus of the project.

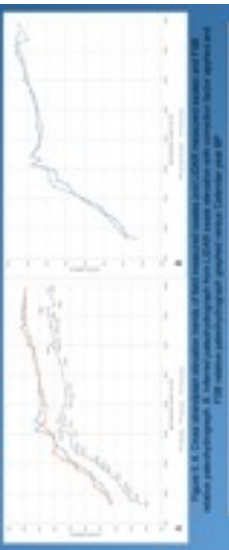


Figure 3. Elevation profile of the Sault Ste. Marie Strandplain. The blue line represents the elevation profile from topography, and the red line represents the elevation profile from LGM1 subsurface stratigraphy. The elevation difference between the two profiles is approximately 100 m.

Abstract:

The Great Lakes are currently at high water levels, which are expected to increase significantly in the future due to climate change. This has led to a growing concern for the potential impacts of high water levels on the Great Lakes basin, including the potential for increased erosion, flooding, and other impacts. This project aims to provide a better understanding of the paleohydrography of the Great Lakes basin, which can help to inform future planning and management efforts.

Objective:

The objective of this project is to compare paleohydrograph reconstructions from topography and subsurface stratigraphy of the Sault Ste. Marie Strandplain (Figure 1). This comparison will allow us to determine if paleohydrographs derived from LGM1 topography can be used as an alternative to paleohydrographs derived from LGM1 stratigraphy.

Goals:

- Reconstruct a paleohydrograph from LGM1 topography
- Reconstruct a paleohydrograph from LGM1 stratigraphy
- Compare the two paleohydrographs for areas that have not been studied

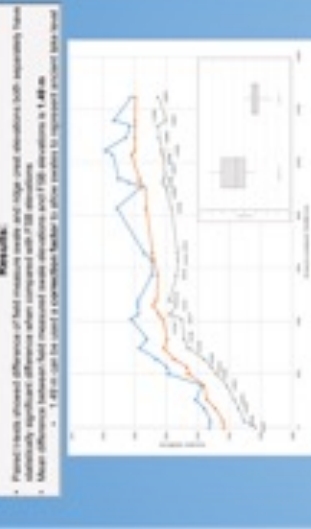


Figure 4. Cross-sectional topographic profile across the strandplain (Figure 1, across 1000 m). The blue line represents the elevation profile from topography, and the red line represents the elevation profile from LGM1 subsurface stratigraphy. The elevation difference between the two profiles is approximately 100 m.

Methods:

- Reconstructing paleohydrographs from topography
- Reconstructing paleohydrographs from subsurface stratigraphy
- Comparing the two paleohydrographs

Results:

- There is a significant difference in elevation between the two profiles, with the topography profile being higher than the LGM1 profile.
- This difference is most pronounced in the central part of the strandplain, where the elevation difference is approximately 100 m.
- The difference in elevation is likely due to subsidence of the strandplain over time, which has led to a lower elevation in the LGM1 profile.

Conclusions:

The results of this project show that paleohydrographs derived from topography and subsurface stratigraphy are not equivalent. This suggests that paleohydrographs derived from topography may not be a reliable alternative to paleohydrographs derived from subsurface stratigraphy.

Methods:

- Reconstructing paleohydrographs from topography
- Reconstructing paleohydrographs from subsurface stratigraphy
- Comparing the two paleohydrographs

Results:

- There is a significant difference in elevation between the two profiles, with the topography profile being higher than the LGM1 profile.
- This difference is most pronounced in the central part of the strandplain, where the elevation difference is approximately 100 m.
- The difference in elevation is likely due to subsidence of the strandplain over time, which has led to a lower elevation in the LGM1 profile.

Conclusions:

The results of this project show that paleohydrographs derived from topography and subsurface stratigraphy are not equivalent. This suggests that paleohydrographs derived from topography may not be a reliable alternative to paleohydrographs derived from subsurface stratigraphy.

Abstract:

The Great Lakes are currently at high water levels, which are expected to increase significantly in the future due to climate change. This has led to a growing concern for the potential impacts of high water levels on the Great Lakes basin, including the potential for increased erosion, flooding, and other impacts. This project aims to provide a better understanding of the paleohydrography of the Great Lakes basin, which can help to inform future planning and management efforts.

Objective:

The objective of this project is to compare paleohydrograph reconstructions from topography and subsurface stratigraphy of the Sault Ste. Marie Strandplain (Figure 1). This comparison will allow us to determine if paleohydrographs derived from LGM1 topography can be used as an alternative to paleohydrographs derived from LGM1 stratigraphy.

Goals:

- Reconstruct a paleohydrograph from LGM1 topography
- Reconstruct a paleohydrograph from LGM1 stratigraphy
- Compare the two paleohydrographs for areas that have not been studied

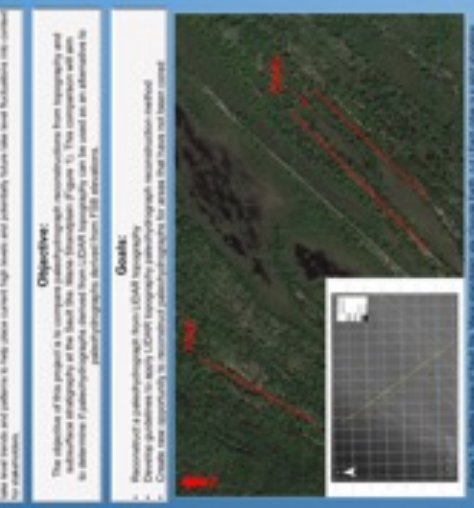


Figure 5. Satellite image of the Sault Ste. Marie Strandplain. The red line indicates the location of the strandplain. The strandplain is a low-lying area that has been submerged by the Great Lakes water. The image also shows the surrounding land and water bodies.

Methods:

- Reconstructing paleohydrographs from topography
- Reconstructing paleohydrographs from subsurface stratigraphy
- Comparing the two paleohydrographs

Results:

- There is a significant difference in elevation between the two profiles, with the topography profile being higher than the LGM1 profile.
- This difference is most pronounced in the central part of the strandplain, where the elevation difference is approximately 100 m.
- The difference in elevation is likely due to subsidence of the strandplain over time, which has led to a lower elevation in the LGM1 profile.

Conclusions:

The results of this project show that paleohydrographs derived from topography and subsurface stratigraphy are not equivalent. This suggests that paleohydrographs derived from topography may not be a reliable alternative to paleohydrographs derived from subsurface stratigraphy.